Advances in Applied Mathematics and Mechanics
Adv. Appl. Math. Mech., Vol. **10**, No. 1, pp. 209-241

DOI: 10.4208/aamm.OA-2016-0063
February 2018

The Static Solution for the Layered Piezoelectric Bounded Domain with Side Face Load by the Modified SBFEM

Shan Lu[1,2], Jun Liu[1,2,3,4,*], Gao Lin[1,2], Zihua Zhang[5] and Pengchong Zhang[1,2]

[1] *State Key Laboratory of Coastal and Offshore Engineering, Dalian University of Technology, Dalian, Liaoning 116024, China*
[2] *School of Hydraulic Engineering, Faculty of Infrastructure Engineering, Dalian University of Technology, Dalian, Liaoning 116024, China*
[3] *Ocean Engineering Joint Research Center of DUT-UWA*
[4] *State Key Laboratory of Structural Analysis for Industrial Equipment, Dalian University of Technology, Dalian, Liaoning 116024, China*
[5] *Faculty of Civil Engineering, Ningbo University, 315211, China*

Received 19 July 2016; Accepted (in revised version) 13 June 2017

Abstract. The static response of two-dimensional horizontal layered piezoelectric bounded domain with side face load was investigated. In this paper, the modified scaled boundary finite element method (SBFEM) is provided as an effective semi analytical methodology. The method is used to solve the static problem for the layered piezoelectric bounded domain. The scaling line definition extends the SBFEM to be more suitable for analyzing the multilayered piezoelectric bounded domain. It avoids the limitations of original SBFEM in modeling the horizontal layered bounded domain. The modified SBFEM governing equation with piezoelectric medium is derived by introducing Duality variable in the Hamilton system. This derivation technology makes the progress be concise. The novel displacement and electric governing equations of the modified SBFEM is given together by the first time. The node forces can be expressed as power exponent function with radial coordinate by introducing the auxiliary variable and using the eigenvalue decomposition. The novel modified SBFEM solution of layered bounded domain with piezoelectric medium is solved. The new power expansion function of layered piezoelectric medium with side face load is proposed. This technology significantly extends the application range of modified SBFEM. The novel treatment of side face load for the layered piezoelectric bounded domain is proposed. Numerical studies are conducted to demonstrate the accuracy of proposed technique in handling with the static problem of layered bounded domain with piezoelectric medium for side face load. The influence of the side face load type and depth are discussed in detail.

*Corresponding author.
Email: liujun8128@126.com (J. Liu)

AMS subject classifications: 60-08

Key words: Modified scaled boundary finite element method, piezoelectric medium, side face load, layered bounded domain.

1 Introduction

The static analysis of the layered bounded domain with piezoelectric medium is an attractive problem, such as the layered piezoelectric plate analysis, sensors application, aerospace panels, structural analysis and fracture mechanics. Because of the excellent piezoelectric material properties, the piezoelectric material was used to the smart structures and small order magnitude model. The widely applications and mathematical challenges characteristics of piezoelectric material has attracted many researchers to study the static analysis of layered piezoelectric model [2, 27]. Therefore, it is worthily to pay attention to the static analysis of layered bounded domain with piezoelectric medium, especially for the horizontal layered piezoelectric model. The piezoelectric material owns excellent ability in elector-mechanical convertibility field. Thus, the piezoelectric analysis becomes a favorite topic in engineering application. However, there are very few analytical solutions and numerical solutions for the horizontal layered bounded domain with piezoelectric medium. Therefore, it has more practical significance to propose a new solution for the static responses of the horizontal layered piezoelectric medium.

The piezoelectric material has excellent material properties. Thus, the electroelastic problem for layered medium has been investigated by many researchers. The piezoelectric material has many advantages, such as the high accuracy, miniaturization and sensitive characteristics. It can be applied to many different fields, such as the electroacoustic transducers, microrobot, atomic force microscope cantilevers and structural fracture mechanics [24, 55]. The piezoelectric material also was extended to model the half space domain problem [3] and the unbounded domain problem [36]. The layered piezoelectric medium widely exists in the nature. The piezoelectric composite structures, such as the layered piezoelectric plates and beams, require the efficient and accurate electromechanical model which has electric and mechanical behaviors. The piezoelectric structures can solve by the coupled equations with electric and mechanical interlaminar continuity conditions and boundary conditions [26]. Exact solutions of the flat panels and rectangular plates with the piezoelectric medium have been obtained [44, 45, 54]. Based on the three dimensional theory of elasticity, the static and free vibration of a cross-ply laminated composite plate in piezoelectric layers has been analyzed [22]. The analytical solutions can be easily solved for the simple model shapes with specified boundary conditions. Therefore, the finite element technology becomes a top priority to analyze the general piezoelectric structures. The finite element piezoelectric model which employs the Hamilton's variational principle has been analyzed [31]. According to the coupled refined high-order global-local theory, a finite element model for the sandwich beams

with piezoelectric layers was built [32]. Several 2D FE piezoelectric models with different assumptions on the mechanical displacement field have been reported [21, 26]. The piezoelectric material which its characteristics vary with the coordinate is defined as the functionally graded piezoelectric material (FGPM), and a large number of studies were focused on this topic. The wave propagation in layered FGPM structure was investigated [8]. The acoustic wave propagation on the shear horizontal surface with layered FGPM was studied [18]. The initial stress causing by the surface wave propagation behavior for the three-layered composite FGPM structure has been reported [48]. The multiple scattering of electro-elastic wave and the dynamic response of FGPM layered structure are discussed in literature [20]. The piezoelectric material can also be applied in thermodynamics field. The fracture problem with piezoelectric layer was investigated [56]. The thermo-elastic analysis for the FGPM spherical layered model was analyzed [4]. The Green's function of anisotropic piezoelectric unbounded domain was investigated [35, 40–42]. By considering the eminent properties of piezoelectric material, the piezoelectric medium is suitable to solve the magnetoelectroelastic problem. The layered half-space with planar transversely isotropic magnetoelectroelastic medium was discussed [38]. The dynamic electromagneto-mechanical response of the clamped-free terfenol laminates was analyzed [39].

For the bounded domain with piezoelectric medium, a large number of literatures have been reported. The electromechanical response of the piezoelectric laminated micro plate which subjects the ultrasonic wave excitation has been discussed [28]. The vibration phenomenon in piezoelectric flexible cantilever plate was studied [43]. The static analysis of functionally graded, anisotropic and linear magneto-electro-elastic plates was investigated by the semi analytical element method [6]. The SH wave propagation depositing on the piezoelectric bounded plates was investigated [14]. The linear piezoelectric plate vibrations were studied [53]. A lot of numerical methods are used to model the layered piezoelectric bounded domain. The equivalent single layer and layerwise approximations have been considered for the piezoelectric layered model. By dividing the layers into many sublayers, the results can satisfy convergence speed and the computational cost is low. A single piezoelectric layer approximation solution can be given by the first-order shear theory [46]. The wave propagation in the periodic piezoelectric layered medium can be found [37]. The anti-plane transverse wave propagation in layered piezoelectric structures was analyzed [10]. The finite element method (FEM) is one of the famous technologies in modeling the static and dynamic analysis of layered piezoelectric problems. The static response of beams with functionally graded piezoelectric medium was analyzed by using the finite element method [19]. The temporal stability of node-based smoothed finite element method (NS-FEM) was used to solve the static and frequency analyses of the piezoelectric medium [12]. The stress singularity analysis of 3D transversely isotropic piezoelectric bonded joints was solved by the Eigen decomposition in FEM [25]. The Rayleigh wave propagation in piezoelectric substrate was analyzed by FEM [1]. One dimensional FEM was employed to solve the static characteristic of the piezoelectric composite beams [30]. However, the disadvantages of FEM also exist. In

order to obtain the accurate solution, the problem domain needs to be dispersed into numbers of elements. Therefore, it leads to the poor computation efficiency for the large scale system. Subsequently, an attracting method which named as the boundary element method (BEM) was proposed to avoid the disadvantages of FEM. In the BEM, only the problem domain boundary needs to be discretized, the dimension is reduced by one, and the mesh generation is greatly simplified. The fundamental solution of BEM bases on the Green's function. The BEM has been applied in many fields, such as the fracture problem, heat conduction problem, wave propagation problem. The fracture analysis of thin piezoelectric structure was studied by developing a 2D time-domain BEM [62]. The three dimensional transient heat conduction in heterogeneity unbounded soil was modelled by BEM [52]. The wave propagation in continuously inhomogeneous half-plane was solved by BEM with closed-form Green's function [23]. By solving the Green's function in frequency-wave number domain, the SH wave propagation for layered elastic half-space was proposed by BEM [47]. However, the fundamental solution is difficult to obtain for the complex problems. In order to analyze the horizontal layered model, the thin layer method (TLM) was investigated [29, 49]. The horizontal layer is divided into many small sublayers in TLM, and then the sublayers are assembled together. The enough accuracy can be achieved in this approximate way. The wave propagation in inhomogeneous piezocomposite layered media which subjected to the mechanical load and electrical excitation was analyzed by TLM [9]. Combining the equations of BEM and TLM, the equations of motion can be formulated in the wavenumber-frequency domain (2.5D domain) [15]. However, the TLM is only suitable for the homogeneous medium with small layer thickness.

A novel semi-analytical numerical technique which named as the scaled boundary finite method (SBFEM) was proposed [50]. This method combines the advantages of BEM and FEM, and the SBFEM has its own special features as well. The problem domain boundary needs to be discretized in the SBFEM, and the spatial dimension is reduced by one. The SBFEM can couple with FEM seamlessly by using the same shape functions, and it is analytical in radial direction, therefore, no fundamental solution and artificial boundary conditions are required. For anisotropic medium, piezoelectric medium and the complex geometry model, the SBFEM can deal with these models without any difficulty. The SBFEM can be applied to model lots of problems successfully, such as the wave propagation in unbounded domain, the singular analysis for bounded domain, non-homogeneous medium and fracture analysis. The nonlinear solution of the SBFEM was applied to the geotechnical structures [11]. The liquid sloshing in horizontal elliptical tanks were solved by the SBFEM [57–59]. The SBFEM also can be used to deal with the dams [60]. The elastic wave propagation in layered medium was studied by SBFEM [13]. The soil-structure interaction problems which involving the semi-infinite layers can be classified into scalar and vector wave propagations. The transient response of non-homogeneous unbounded domain with varying elasticity modulus and mass density was analyzed by SBFEM [5]. The SBFEM was employed to two-dimensional fracture analysis with piezoelectric medium [33]. The displacement and electric potential, stress

and electric displacement of any point in the domain can be obtained analytically. The SBFEM is used to solve the static and dynamic stress intensity factors (SIFs) [61]. The fully-automatic modeling technology for static problem and the series-increasing solution for dynamic problem were developed. The three-dimensional seismic SSI analysis which bases on the substructure method was investigated by coupling the FEM and SBFEM [51]. The mixed SBFEM formulation for the nearly incompressible linear multi-materials was proposed [34].

The scaling center definition is required in original SBFEM, and the radial lines radiated from scaling center to boundary. For modelling the horizontal layered domain, the scaling center has to be sited in the infinite. And, this leads to the included angle between the adjacent radial lines is equal to zero approximately. To overcome the limitation of original SBFEM in analyzing the horizontal layered model, a modified scaled boundary finite element method was proposed to solve the three-dimensional elastodynamic unbounded domain problem [7]. In the modified SBFEM, the original scaled center is replaced by a scaling line which is vertical to the horizontal layers. Thus, the modified SBFEM can successfully simulate the horizontal layered unbounded domain without any difficulty. In original SBFEM, the bounded domain has to be divided into several subdomains which are suitable for analyzing the complex multilayered model. The disadvantage of original SBFEM is avoided by introducing the scaling line definition. The multilayered model can be directly computed. In this paper, the modified SBFEM is proposed to analyze the horizontal layered bounded domain with piezoelectric medium. Firstly, the two-dimensional static governing equation of piezoelectric medium is given. Then, the generalized stress strain relationship of piezoelectric material is expressed. According to the above preparation work, the Duality theory is used in Hamilton system for deriving the modified SBFEM governing equation. The modified SBFEM state equation which contains the displacement and electric responses of piezoelectric medium is obtained. The Hamilton derivation technology makes the progress more concisely. Secondly, the modified SBFEM equation for piezoelectric medium is solved by eigenvalue decomposition. By introducing the auxiliary variable, the generalized displacement and node forces can be expressed as power exponent function with radial coordinate. As so far, the modified SBFEM static solution for layered piezoelectric bounded domain is obtained. The displacement and electric charge for the arbitrary internal nodes can compute through the shape function in circumferential scaled boundary coordinate η. When the external force subjects on the radial lines, the SBFEM equation needs to be treated specially. For the SBFEM model, the radial boundaries of problem domain are known as side faces. A technique was given in SBFEM allowing displacements to be prescribed along side faces [16]. This technique significantly extends the application range of SBFEM in elastostatic filed. In this paper, the modified SBFEM is extended to solve the piezoelectric layered bounded domain subjecting side face load. The side face load and displacements mode were expressed by power function of radial coordinate [17]. A novel side face load formulation for the modified SBFEM is proposed in this paper. The side face load can be expressed as the power exponent function with the radial coordinate. And this new

technology makes the horizontal layered bounded domain can be analyzed directly. The generalized displacement and node forces can be assembled by the general solution for boundary load case and the special solution for side face load case.

The two-dimensional modified SBFEM for the piezoelectric material is built in Section 2. The elastic-electric governing equation for piezoelectric medium is given firstly. Then, the geometry coordinates transformation of the modified SBFEM in piezoelectric medium is proposed. Because there is electric freedom for piezoelectric medium, the geometry coordinates transformation for the proposed method is novel and different from those of the original SBFEM and modified SBFEM. Based on the Hamiltonian derivation technology, the modified SBFEM state equation for displacement and electric is formulated in Section 3. In Section 4, the static solution for layered piezoelectric bounded domain is computed. In Section 5, the side face load case is considered. A novel side face load form is proposed in modified SBFEM. In Section 6, numerical examples are revealed to demonstrate the accuracy of proposed method. In the Section 7, the conclusions are remarked.

2 The modified scaled boundary finite method for piezoelectric medium

The static analysis for horizontal layered bounded domain with piezoelectric medium is an interesting topic. The modified SBFEM is proposed to deal with the horizontal layered piezoelectric problem. The scaling center of original SBFEM is replaced by scaling line, and the horizontal layers can be directly model with no problem. Firstly, the two-dimension static governing equations for piezoelectric medium are described. Then, the SBFEM coordinate transform is introduced.

2.1 Two-dimensional static governing equations for the piezoelectric material

The two-dimensional governing equations for piezoelectric medium are listed as follows, and the body load and free electric charge are ignored

$$\{\sigma\} = [c]\{\varepsilon\} - [e]^T\{E\}, \tag{2.1a}$$

$$\{D\} = [e]\{\varepsilon\} + [p]\{E\}, \tag{2.1b}$$

where, $\{\sigma\}$, $\{\varepsilon\}$ and $\{D\}$ are the stress vector, strain vector and electric displacement vector, respectively. $\{E\}$ is electric field, $[c]$ are elastic constants, $[e]$ are piezoelectric constants, and $[p]$ are permittivities. By assembling Eqs. (2.1a) and (2.1b), the governing equation for piezoelectric medium can be expressed as following:

$$\{\bar{\sigma}\} = [H]\{\bar{\varepsilon}\}, \tag{2.2}$$

in which, the stress and electric displacement are combined as $\{\bar{\sigma}\}=[\sigma_{xx},\sigma_{yy},\sigma_{xy},D_x,D_y]^T$, the corresponding strain and electric are combined as as $\{\bar{\varepsilon}\}=[\varepsilon_{xx},\varepsilon_{yy},\gamma_{xy},-E_x,-E_y]^T$. The material constant matrix $[H]$ can be given as

$$[H]=\begin{bmatrix} c_{11} & c_{13} & 0 & 0 & e_{31} \\ c_{13} & c_{33} & 0 & 0 & e_{33} \\ 0 & 0 & c_{44} & e_{15} & 0 \\ 0 & 0 & e_{15} & -p_{11} & 0 \\ e_{31} & e_{33} & 0 & 0 & -p_{33} \end{bmatrix}. \tag{2.3}$$

The plane-strain problem is considered in this paper. Then, the expression of generalized strain $\{\bar{\varepsilon}\}$ can be denoted as following

$$\{\bar{\varepsilon}\}=[L]\{\bar{u}\}=[L]\{u_x,u_y,\phi\}^T, \tag{2.4}$$

where, u_x,u_y are the x-direction and y-direction displacement components, ϕ denoted as electric potential, and $[L]$ is the linear partial differential operator

$$[L]=\begin{bmatrix} \dfrac{\partial}{\partial\hat{x}} & 0 & \dfrac{\partial}{\partial\hat{y}} & 0 & 0 \\ 0 & \dfrac{\partial}{\partial\hat{y}} & \dfrac{\partial}{\partial\hat{x}} & 0 & 0 \\ 0 & 0 & 0 & \dfrac{\partial}{\partial\hat{x}} & \dfrac{\partial}{\partial\hat{y}} \end{bmatrix}^T. \tag{2.5}$$

According to the interaction force principle, the governing equation for the elastostatic and electrostatic problem is given as follow

$$[L]^T\{\bar{\sigma}\}+\{\bar{f}\}=0, \tag{2.6}$$

where, the generalized node force is denoted as $\{\bar{f}\}=[f_{bx},f_{by},q_b]^T$. f_{bx} and f_{by} are mechanical body forces, q_b is electric body force.

2.2 The modified scaled boundary geometry coordinate transformation

As shown in Fig. 1, a horizontal layered bounded domain is described in this example. The boundaries are denoted as L. The interfaces of two adjacent layers are assumed horizontal. The displacements and tractions are continuous on interfaces. Two scaled boundary coordinates η and ξ are introduced to describe the surface circumferential direction and radial direction. As shown in Fig. 1(b), the boundary node coordinate and inside node coordinate are denoted as $(\hat{x},\hat{y})$ and (x,y) in the two-dimensional Cartesian coordinate system. In the modified SBFEM, a vertical line-the scaling line replaces traditional scaling centre, and the scaling line coincides with $\hat{y}$ axis in Fig. 1(b). The modified

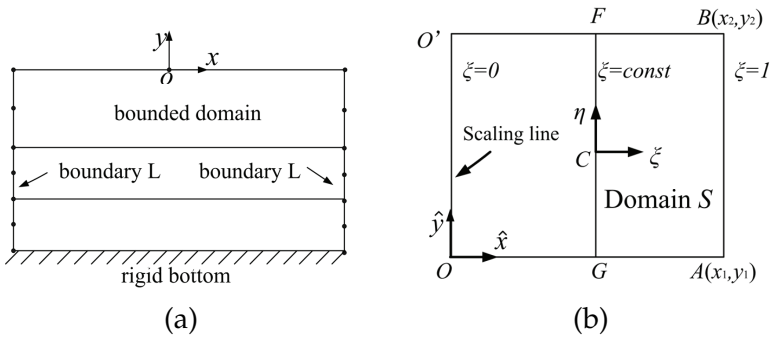

Figure 1: Modified scaled boundary finite element method for 2D layered medium. (a) 2D layered medium (b) Coordinate transformation of the bounded domain model.

SBFEM inherits the advantages of SBFEM. Thus, the boundary needs to be discretized and the dimension of problem domain is reduced by one. For bounded domain, the radial coordinate which is parallels to x-axis runs from scaling line to boundary. The radial coordinate ranges are given as follows: $\xi=1$ on the domain boundary, $0\leq\xi\leq1$ for bounded domain and $\xi\geq1$ for unbounded domain. The shape functions $[N(\eta)]$ are used to interpolate a series of parallel lines in the dimensionless coordinate direction. As shown in Fig. 1(b), the bounded domain is composed by the lines which are parallel to $\hat{x}$ axis and pass through scaling line. By scaling the factor ξ, bounded domain S can be described. It is interesting to note that the vertical coordinates are retained.

For fixed radial coordinate ξ, the arbitrary Cartesian node coordinate $(\hat{x},\hat{y})$ can be obtained by interpolating the space node coordinate $(\{x\},\{y\})$ by using shape function $[N(\eta)]$. As shown in Fig. 1(b), the arbitrary line FG $(\xi=const)$ is parallel to the scaling line OO' and boundary line AB. Thus, the node coordinates can be obtained according to the similarity. The modified scaled boundary coordinate transformation is expressed as following:

$$\begin{cases}\hat{x}(\xi,\eta)=[N(\eta)]\hat{x}(\xi)=\xi[N(\eta)\{x\},\\ \hat{y}(\xi,\eta)=[N(\eta)]\hat{y}(\xi)=[N(\eta)]\{y\}.\end{cases}\tag{2.7}$$

The generalized displacement and stress components are unchanged in Cartesian coordinate system. The partial derivatives with respect to scaled boundary coordinates are formulated as following:

$$\begin{Bmatrix}\partial/\partial\xi\\ \partial/\partial\eta\end{Bmatrix}=[\hat{J}(\xi,\eta)]\begin{Bmatrix}\partial/\partial\hat{x}\\ \partial/\partial\hat{y}\end{Bmatrix},\tag{2.8}$$

where $[\hat{J}(\varepsilon,\eta)]$ denoted as Jacobian matrix

$$[\hat{J}(\xi,\eta)]=\begin{bmatrix}\hat{x}_{,\xi} & \hat{y}_{,\xi}\\ \hat{x}_{,\eta} & \hat{y}_{,\eta}\end{bmatrix}=\begin{bmatrix}x & 0\\ 0 & y_{,\eta}\end{bmatrix}=[J],\tag{2.9}$$

in which $[J]$ is the boundary Jacobian matrix. By using the partial derivative in Eq. (2.8), the partial derivatives with respect to Cartesian coordinates can be expressed to the partial derivatives with modified scaled boundary coordinates, as given in Eq. (2.10)

$$\begin{Bmatrix}\partial/\partial\hat{x}\\ \partial/\partial\hat{y}\end{Bmatrix}=[\hat{J}(\xi,\eta)]^{-1}\begin{Bmatrix}\partial/\partial\xi\\ \partial/\partial\eta\end{Bmatrix}=\frac{1}{|J|}\begin{Bmatrix}y_{,\eta}\\ 0\end{Bmatrix}\frac{\partial}{\partial\xi}+\frac{1}{|J|}\begin{Bmatrix}0\\ x\end{Bmatrix}\frac{\partial}{\partial\eta}, \tag{2.10}$$

with $|J|$ is the value of determinant.

To analyze the plane problem, the normal stress vectors $\{t^{\xi}\}$ and $\{t^{\eta}\}$ on line S^{ε} and S^{η} are formulated as following:

$$\{t^{\xi}\}=\frac{|J|}{g^{\xi}}[b^1]^T\{\sigma\},\quad \{t^{\eta}\}=\frac{|J|}{g^{\eta}}[b^2]^T\{\sigma\}, \tag{2.11}$$

where $g^{\xi}=y$, $g^{\eta}=x$. For $\xi=const$, the length of infinitesimal arc is expressed as

$$d\Gamma^e=\sqrt{(x_{,\eta})^2+(y_{,\eta})^2}d\xi=|y_{,\eta}|\,d\xi. \tag{2.12}$$

The linear partial differential operator $[L]$ with the scaled boundary coordinates ξ and η is rewritten as following

$$[L]=[b^1]\frac{\partial}{\partial\xi}+[b^2]\frac{\partial}{\partial\eta} \tag{2.13}$$

with

$$[b^1]=\frac{1}{|J|}\begin{bmatrix}y_{,\eta}&0&0\\0&0&0\\0&y_{,\eta}&0\\0&0&y_{,\eta}\\0&0&0\end{bmatrix}, \tag{2.14a}$$

$$[b^2]=\frac{1}{|J|}\begin{bmatrix}0&0&0\\0&x&0\\x&0&0\\0&0&0\\0&0&x\end{bmatrix}. \tag{2.14b}$$

By taking account for the electric potential contribution, the matrixes $[b^1]$ and $[b^2]$ with the dimensions 5×3 are different from those of the original SBFEM. Similarly the form of Eq. (2.7), the generalized displacement $\{\bar{u}(\xi,\eta)\}$, which contains displacement and electric potential can be discretized by using shape function $[N(\eta)]$ and weight function $\{w\}$

$$\{\bar{u}(\xi,\eta)\}=[N(\eta)]\{\bar{u}(\xi)\},\quad \{w(\xi,\eta)\}=[N(\eta)]\{w(\xi)\}. \tag{2.15}$$

According to Eqs. (2.4), (2.13) and (2.15), the generalized strains $\{\bar{\varepsilon}\}$ is formulated as described in Eq. (2.16) with respect to the generalized displacement $\{\bar{u}\}$

$$\{\bar{\varepsilon}\}=[B^1]\{\bar{u}\}_{,\xi}+[B^2]\{\bar{u}\} \tag{2.16}$$

with

$$[B^1]=[b^1][N(\eta)],\quad [B^2]=[b^2][N(\eta)]_{,\eta}. \tag{2.17}$$

It is worthy to note that, the matrixes $[B^1]$ and $[B^2]$ only depend on the bounded domain boundary condition. Substituting Eq. (2.15) into the generalized stress and strain governing Eq. (2.2), the generalized stresses $\{\bar{\sigma}\}$ is denoted as

$$\{\bar{\sigma}\}=[H][B^1]\{\bar{u}\}_{,\xi}+[H][B^2]\{\bar{u}\}. \tag{2.18}$$

3 Hamiltonian derivation of the displacement and electric modified SBFEM equation

In this paper, the displacement and electric potential governing equation of modified SBFEM is presented. Based on Duality system theory, the Hamiltonian variational principle is applied to be compatible with n order Hamilton system. This technology is applied to derivate the modified SBFEM governing equation. Then, the Lagrangian density function $L(\{u\},\{\dot{u}\})$, which is the summation of strain energy density function and work of external force, is introduced to Hamiltonian variational principle. By using Legendre transformation, the dual variable $\{q\}$ of generalized stress is formulated as following

$$\{q\}=\partial L/\partial\dot{u}. \tag{3.1}$$

The Hamiltonian function H can be formulated as follow

$$H(\{u\},\{q\})=\{q\}^T\{\dot{u}\}-L(\{u\},\{\dot{u}\}). \tag{3.2}$$

According to the Hamiltonian variational principle, yielded that

$$\delta\int_{z_0}^{z_1}[\{q\}^T\{u\}-H(\{u\},\{q\})]dz=0. \tag{3.3}$$

The partial derivatives are obtained are given in the following forms

$$\{\dot{u}\}=\partial H/\partial q,\quad \{\dot{q}\}=-\partial H/\partial u. \tag{3.4}$$

According to the above introduction for Hamiltonian method, the Lagrangian density function $L(\{\bar{u}\},\{\dot{\bar{u}}\})$ for piezoelectric medium can be constituted firstly. The generalized

strain energy density function U is formulated as following

$$\begin{aligned}U&=\int_S\frac{1}{2}\{\bar{\sigma}\}^T\{\bar{\varepsilon}\}dS=\int_S\frac{1}{2}\{\bar{\varepsilon}\}^T[\mathrm{H}]\{\bar{\varepsilon}\}dxdy\\&=\int_{\xi_0}^{\xi_1}\int_{\eta_0}^{\eta_1}\frac{1}{2}([\mathbf{B^1}]\{\bar{u}\}_{,\xi}+[\mathbf{B^2}]\{\bar{u}\})^T[\mathrm{H}]([\mathbf{B^1}]\{\bar{u}\}_{,\xi}+[\mathbf{B^2}]\{\bar{u}\})|J|d\eta d\xi\\&=\int_{\xi_0}^{\xi_1}\int_{\eta_0}^{\eta_1}\frac{1}{2}(\{\bar{u}\}_{,\xi}^T[\mathbf{B^1}]^T[\mathrm{H}][\mathbf{B^1}]\{\bar{u}\}_{,\xi}+\{\bar{u}\}_{,\xi}^T[\mathbf{B^1}]^T[\mathrm{H}][\mathrm{B}^2]\{\bar{u}\}\\&\quad+\{\bar{u}\}^T[\mathrm{B}^2]^T[\mathrm{H}][\mathrm{B}^1]\{\bar{u}\}_{,\xi}+\{\bar{u}\}^T[\mathrm{B}^2]^T[\mathrm{H}][\mathrm{B}^2]\{\bar{u}\})|J|d\eta d\xi\\&=\int_{\xi_0}^{\xi_1}\frac{1}{2}(\{\bar{u}\}_{,\xi}{}^T[\mathrm{E}^0]u_{,\xi}+\{\bar{u}\}_{,\xi}{}^T[\mathrm{E}^1]^T\{\bar{u}\}+\{\bar{u}\}^T[\mathrm{E}^1]\{\bar{u}\}_{,\xi}+\{\bar{u}\}^T[\mathrm{E}^2]\{\bar{u}\})d\xi.\end{aligned}\tag{3.5}$$

For convenient, the coefficient matrices $[E^0]$, $[E^1]$ and $[E^2]$ are introduced, they only relate to boundary elements

$$[E^0]=\int_{-1}^{+1}[B^1]^T[H][B^1]|J|d\eta,\tag{3.6a}$$

$$[E^1]=\int_{-1}^{+1}[B^2]^T[H][B^1]|J|d\eta,\tag{3.6b}$$

$$[E^2]=\int_{-1}^{+1}[B^2]^T[H][B^2]|J|d\eta.\tag{3.6c}$$

Because the surface tractions and body forces are ignored in this study, the work causing by external force is equal to zero

$$W=0.\tag{3.7}$$

For the static electromechanical system, the radial direction coordinate ξ is selected as time-axis. Therefore, $\{\dot{u}\}$ can be represented as $\{\dot{u}\}=\partial\bar{u}/\partial\xi$. According to the definition of Lagrangian density function, $L(\{\bar{u}\},\{\dot{u}\})$ for piezoelectric medium can be expressed as

$$\begin{aligned}&L(\{\bar{u}\},\{\bar{u}\}_{,\xi})=U-W\\&=\frac{1}{2}\Big(\{\bar{u}\}_{,\xi}{}^T[\mathrm{E}^0]\{\bar{u}\}_{,\xi}+\{\bar{u}\}_{,\xi}{}^T[\mathrm{E}^1]^T\{\bar{u}\}+\{\bar{u}\}^T[\mathrm{E}^1]\{\bar{u}\}_{,\xi}+\{\bar{u}\}^T[\mathrm{E}^2]\{\bar{u}\}\Big).\end{aligned}\tag{3.8}$$

Applying the Legendre transformation, the dual vector $\{\bar{q}\}$ can be given as follow

$$\{\bar{q}\}=\frac{\partial L}{\partial\bar{u}_{,\xi}}=[E^0]\{\bar{u}\}_{,\xi}+[E^1]^T\{\bar{u}\}.\tag{3.9}$$

Because of matrix $[E^0]$ is symmetry and positive definite, and above equation can be rewritten as

$$\{\bar{u}\}_{,\xi}=[E^0]^{-1}(\{\bar{q}\}-([E^1])^T\{\bar{u}\})=[E^0]^{-1}\{\bar{q}\}-[E^0]^{-1}[E^1]^T\{\bar{u}\}.\tag{3.10}$$

Based on the expressions for dual vectors $(\{\bar{u}\},\{\bar{q}\})$ and Lagrangian density function in Eq. (3.6), the Hamiltonian function can be devoted as

$$\begin{aligned}
&H(\{\bar{u}\},\{\bar{q}\})\\
=&\{\bar{q}\}^T\{\bar{u}\}_{,\xi}-L(\{\bar{u}\},\{\bar{u}\}_{,\xi})\\
=&\{\bar{q}\}^T\{\bar{u}\}_{,\xi}-\frac{1}{2}(\{\bar{u}\}_{,\xi}^T[E^0]\{\bar{u}\}_{,\xi}+\{\bar{u}\}_{,\xi}{}^T[E^1]^T\{\bar{u}\}+\{\bar{u}\}^T[E^1]\{\bar{u}\}_{,\xi}+\{\bar{u}\}^T[E^2]\{\bar{u}\})\\
=&\frac{1}{2}(\{\bar{u}\}_{,\xi}^T[E^0]\{\bar{u}\}_{,\xi}-\{\bar{u}\}^T[E^2]\{\bar{u}\}).
\end{aligned}\tag{3.11}$$

Substituting the partial derivative Eq. (3.10) into the Hamiltonian function Eq. (3.11) yielded that

$$\begin{aligned}
&H(\{\bar{u}\},\{\bar{q}\})\\
=&\frac{1}{2}\Big([E^0]^{-1}\{\bar{q}\}-[E^0]^{-1}[E^0]^T\{\bar{u}\}\Big)^T[E^0]\Big([E^0]^{-1}\{\bar{q}\}-[E^0]^{-1}[E^1]^T\{\bar{u}\}\Big)-\frac{1}{2}\{\bar{u}\}^T[E^2]\{\bar{u}\}\\
=&\frac{1}{2}(\{\bar{q}\}^T[E^0]^{-T}\{\bar{q}\}-\{\bar{u}\}^T[E^1][E^0]^{-T}\{\bar{q}\}-\{\bar{q}\}^T[E^0]^{-T}[E^1]^T\{\bar{u}\}\\
&+\{\bar{u}\}^T[E^1][E^0]^{-T}[E^1]^T\{\bar{u}\})-\frac{1}{2}\{\bar{u}\}^T[E^2]\{\bar{u}\}\\
=&\frac{1}{2}\{\bar{q}\}^T[E^0]^{-T}\{\bar{q}\}-\{\bar{q}\}^T[E^0]^{-T}[E^1]^T\{\bar{u}\}+\frac{1}{2}\{\bar{u}\}^T([E^1][E^0][E^1]^T-[E^2])\{\bar{u}\}.
\end{aligned}\tag{3.12}$$

By applying the Hamiltonian variational principle, the Hamilton canonical equations for piezoelectric medium can be given as following

$$\{\bar{q}\}_{,\xi}=-\partial H/\partial\bar{u}=[E^1][E^0]^{-1}\{\bar{q}\}-([E^1][E^0]^{-T}[E^1]^T-[E^2])\{\bar{u}\},\tag{3.13a}$$

$$\{\bar{u}\}_{,\xi}=\partial H/\partial q=[E^0]^{-T}\{\bar{q}\}-[E^0]^{-T}[E^1]^T\{\bar{u}\}.\tag{3.13b}$$

Substituting the dual vector expression formulation in Eq. (3.9) to the partial derivation Eqs. (3.13a) and (3.13b), the state governing equation of modified SBFEM for piezoelectric medium can be given as following:

$$\begin{Bmatrix}\{\bar{u}\}_{,\xi}\\ \{\bar{q}\}_{,\xi}\end{Bmatrix}=\begin{bmatrix}-[E^0]^{-T}[E^1]^T & [E^0]^{-T}\\ -([E^1][E^0]^{-T}[E^1]^T-[E^2]) & [E^1][E^0]^{-1}\end{bmatrix}\begin{Bmatrix}\{\bar{u}\}\\ \{\bar{q}\}\end{Bmatrix}.\tag{3.14}$$

The state Eq. (3.12) can be abbreviated as

$$\{X(\xi)\}_{,\xi}=[Z]\{X(\xi)\}\tag{3.15}$$

with

$$[X(\xi)]=\begin{bmatrix}\{u(\xi)\}\\ \{q(\xi)\}\end{bmatrix},\quad [Z]=\begin{bmatrix}-[E^0]^{-T}[E^1]^T & [E^0]^{-T}\\ -([E^1][E^0]^{-T}[E^1]^T-[E^2]) & [E^1][E^0]^{-1}\end{bmatrix}.\tag{3.16}$$

The coefficient matrix $[Z]$ is Hamiltonian matrix, and Eq. (3.14) is the governing equation of modified SBFEM for piezoelectric medium. The detailed solving progress can be exhibited in the following section.

4 The static solution of the modified SBFEM governing equation for piezoelectric medium

The matrix function method is applied in solving progress. The advantage of this method is that it can obtain the displacement and stress solutions once time. Firstly, the Hamiltonian matrix $[Z]$ can be eigenvalue decomposed as follow

$$[Z][V]=[V][\Lambda], \tag{4.1}$$

in which the matrices $[V]$, $[\Lambda]$ are the eigenvector and eigenvalue of Hamiltonian matrix $[Z]$, respectively. And the diagonal matrix $[\Lambda]$ can be presented as following:

$$[\Lambda]=\begin{bmatrix}[-\lambda_j] & \\ & [\lambda_j]\end{bmatrix}, \quad j=1,2,\cdots,n, \tag{4.2}$$

with $Re(\lambda_j)<0$, and the eigenvalue is rearranged in descending order. The eigenvector matrix $[V]$ can be blocked arrangement as described in Eq. (4.3) according to eigenvalue form

$$[V]=\begin{bmatrix}[V_{11}] & [V_{12}] \\ [V_{21}] & [V_{22}]\end{bmatrix}. \tag{4.3}$$

The eigenvector matrix can be composed by n column modal displacement vectors. The constant vector $\{c\}$ is introduced to represent the contribution of each mode. The constant vector only depends on boundary conditions. Therefore, the solution of first order ordinary differential Eq. (3.15) can be formulated as following:

$$\{X(\xi)\}=[X(\xi)]\{c\}. \tag{4.4}$$

Defining the auxiliary variable $[Y(\xi)]$ yielded

$$[Y(\xi)]=[V]^{-1}[X(\xi)]. \tag{4.5}$$

Rearranging Eq. (4.5), yielded

$$[X(\xi)]=[V][Y(\xi)]. \tag{4.6}$$

Substituting Eq. (4.5) into Hamiltonian governing Eq. (3.15), one can obtain

$$[Y(\xi)]_{,\xi}=[\Lambda][Y(\xi)]. \tag{4.7}$$

The solution of the first order differential Eq. (4.7) can be given as follow

$$[Y(\xi)]=e^{[\Lambda]\xi}. \tag{4.8}$$

Combining the solution forms in Eqs. (4.6), (4.8) and (4.4), the double variables solution can be solved as

$$\{X(\xi)\}=[V]e^{[\Lambda]\xi}\{c\}. \tag{4.9}$$

For concise, Eq. (4.9) is written in bock matrix form, as following

$$\{X(\xi)\}=\begin{bmatrix}[V_{11}] & [V_{12}]\\ [V_{21}] & [V_{22}]\end{bmatrix}\begin{bmatrix}e^{[-\lambda_j]\xi} & \\ & e^{[\lambda_j]\xi}\end{bmatrix}\begin{Bmatrix}\{c_1\}\\ \{c_2\}\end{Bmatrix}. \tag{4.10}$$

Expanding the solution expressed in Eq. (4.10), the generalized modal displacements and the equivalent model node forces can be formulated as following

$$\{\bar{u}(\xi)\}=[V_{11}]e^{[-\lambda_j]\xi}\{c_1\}+[V_{12}]e^{[\lambda_j]\xi}\{c_2\}, \tag{4.11a}$$

$$\{\bar{q}(\xi)\}=[V_{21}]e^{[-\lambda_j]\xi}\{c_1\}+[V_{22}]e^{[\lambda_j]\xi}\{c_2\}. \tag{4.11b}$$

The generalized displacement for bounded domain is a finite value. Thus, when the eigenvalue $\lambda_j\to\infty$, the displacement $\{u(\xi)\}\to\infty$. Therefore, the integral constant vector is equal to $\{c_2\}=0$. The generalized displacements and equivalent node forces in Eqs. (4.11a) and (4.11b) can be formulated as following:

$$\{\bar{u}(\xi)\}=[V_{11}]e^{[-\lambda_j]\xi}\{c_1\}, \tag{4.12a}$$

$$\{\bar{q}(\xi)\}=[V_{21}]e^{[-\lambda_j]\xi}\{c_1\}. \tag{4.12b}$$

For arbitrary generalized displacement $\{\bar{u}(\xi)\}$, the integration constant vector $\{c_1\}$ is required to satisfy Eq. (4.12a). The solution forms in Eq. (4.12) is novel and firstly proposed in modified SBFEM. Therefore, the integration constant vector $\{c_1\}$ can be obtained by boundary generalized displacement and its formulation is expressed as follow

$$\{c_1\}=\left([V_{11}]e^{[-\lambda_j]}\right)^{-1}\{\bar{u}(\xi=1)\}. \tag{4.13}$$

Substituting Eq. (4.13) into Eq. (4.12b), the generalized equivalent forces $\{\bar{q}(\xi)\}$ on boundary can be written as following

$$\{\bar{q}\}=[V_{21}][V_{11}]^{-1}\{\bar{u}(\xi=1)\}. \tag{4.14}$$

Combining Eqs. (4.12a) and (4.12b), and then canceling the integration constant vector $\{c_1\}$, the boundary static stiffness matrix of bounded domain can be obtained as following

$$[K]=[V_{21}][V_{11}]^{-1}. \tag{4.15}$$

Substituting the generalized displacement (Eq. (4.12a)) into generalized stresses formulation (Eq. (2.18)) yields the stress expression as following:

$$\{\bar{\sigma}(\xi,\eta)\}=[H]\sum_{i=1}^{n}c_i e^{-\lambda_i\xi}([B^2]-\lambda_i[B^1])\{\phi_i\}. \tag{4.16}$$

5 The side face loads solution of the piezoelectric bounded domain

The body loads and side face loads are not discussed in above sections. Therefore, Eq. (3.15) is a homogeneous first order ordinary differential equation without considering side face loads. And, this equation is the static governing equation for piezoelectric layered bounded domain. As innovation, the non-zero side face loads are considered for layered medium. As described in Fig. 2, only the boundary $\xi=1$ is descreted, and the side faces don't need to descrete. Therefore, the nodes only exist on boundary. When the external force acts on boundary, the solutions can be easily obtained as above sections. Here, the side face is defined as the line passes from scaling line to boundary along radial line (as shown in Fig. 2). When the external force acts on side face, the solutions need to be special treated. The additional external virtual work term will appear when there is a non-zero side face load subjecting on side face. For modeling side face loads, the load amplitude should be the function of scaled boundary coordinate ξ. For bounded domain $0\leq\xi\leq1$. Due to the existence of side face load, the non homogeneous term is added to the state governing equation of modified SBFEM (Eq. (3.15)), yielded

$$\{X(\xi)\}_{,\xi}=[Z]\{X(\xi)\}+\{F(\xi)\} \tag{5.1}$$

with the $\{F(\xi)\}=\{F^b(\xi)\}+\{F^t(\xi)\}$, superscripts "$b$" and "$t$" denoted as body loads and side face loads, respectively. The side face loads $\{F^t(\xi)\}=[F_t(\xi),0]^T$, and body loads are absent in this paper.

The solution of non homogeneous differential equation can be sought as the two parts combinations, the general solution of homogeneous Eq. (3.15) and the particular solution of non-homogeneous Eq. (5.1). The general solution (Eqs. (4.12a) and (4.12b)) has been obtained in Section 4. In this section, the key point is to solve additional solution. Many practical loads can be simplified as a series of power function with radial coordinate ξ. As usual, the constant loads or linearly varying loads are considered. In this paper, the side face loads are proposed by the form Eq. (5.2). Comparing the original side face load form $\{F_t(\xi)\}=\xi^t\{F_t\}$ in original SBFEM [55], the proposed side face load form is quite

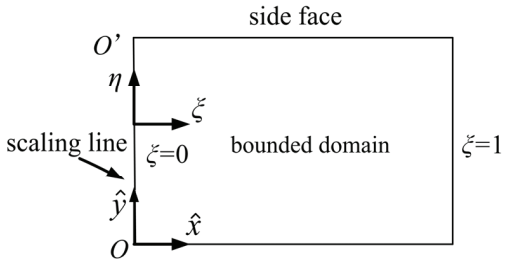

Figure 2: Bounded domain with side face load.

different and novel, as following:

$$\{F_t(\xi)\}=e^{\xi t}\{F_t\}, \tag{5.2}$$

where, t is a arbitrary constant, $\{F_t\}$ is the constant amplitude of side face loads.

The displacement modes for the side face loads case can be expressed as the following form

$$\{u_t(\xi)\}=e^{\xi t}\{\phi_t\}. \tag{5.3}$$

Substituting the displacement modes formulation Eq. (5.3) into the first line of governing Eq. (5.1), yielded

$$[t^2[E^0]+([E^1]^T-[E^1])t-[E^2]]\{\phi_t\}+\{F_t\}=0. \tag{5.4}$$

Then, the mode of side face loads can be obtained by rearrangement as follow

$$\{\phi_t\}=-[t^2[E^0]+([E^1]^T-[E^1])t-[E^2]]^{-1}\{F_t\}. \tag{5.5}$$

Substituting Eq. (5.3) into the second line of Eq. (5.1), the generalized equivalent nodal forces can be obtained as follow

$$\{\bar{q}_t\}=([E^0]te^t+[E^1]^Te^t)\{\phi_t\}. \tag{5.6}$$

Therefore, the complete solution of non homogeneous differential Eq. (5.1) can be given, the solution can be formulated by the following form

$$\{\bar{u}(\xi,\eta)\}=[N(\eta)]\Big(e^{t\xi}\{\phi_t\}+\sum_{i=1}^{n}c_ie^{-\lambda_i\xi}\{\phi_i\}\Big), \tag{5.7}$$

where, $\{\phi_i\}$ is the column vector of matrix $[\Phi]$ ($[\Phi]=[V_{11}]$). For a given set of integration constant vector $\{c\}$, the boundary displacement in Eq. (5.7) can be rewritten in matrix form

$$\{\bar{u}\}=e^t\{\phi_t\}+[\Phi][e^{-\lambda_i}]\{c\}. \tag{5.8}$$

The integration constant vector can be computed by rearranging Eq. (5.8), yielded

$$\{c\}=([\Phi][e^{-\lambda_i}])^{-1}(\{\bar{u}\}-e^t\{\phi_t\}). \tag{5.9}$$

The generalized equivalent forces also can be expressed in matrix form

$$\{\bar{q}\}=\{\bar{q}_t\}+[Q][e^{-\lambda_i}]\{c\} \tag{5.10}$$

with $[Q]=[V_{21}]$.

Substituting Eq. (5.9) into Eq. (5.10) and rewritten the formulation, yields that

$$[Q][e^{-\lambda_i}]([\Phi][e^{-\lambda_i}])^{-1}(\{u\}-e^t\{\phi_t\})=\{q\}-\{q_t\} \tag{5.11}$$

or

$$[K]\{\bar{u}\}=\{\bar{q}\}-\{\bar{q}_t\}+[K]e^t\{\phi_t\}, \tag{5.12}$$

where

$$[K]=[Q][\Phi]^{-1}. \tag{5.13}$$

The equation forms for Eq. (5.13) and Eq. (4.15) are same. It illustrates that the homogeneous equation solution is a part of non homogeneous equation solution. According to boundary conditions of discretized boundaries, the constraint conditions are applied to the column vector of generalized displacement $\{\bar{u}\}$ and nodal forces $\{\bar{q}\}$. The solution process is similar to the usual manner. As so far, the complete boundary displacements for side face load case are obtained. Then, the integration constant vector is acquired by applying Eq. (5.9).

Substituting Eq. (5.7) into Eq. (2.18), the generalized stress for side face load case can be formulated as follow

$$\{\bar{\sigma}(\xi,\eta)\}=[H](e^{t\xi}(t[B^1]+[B^2])\{\phi_t\}+\sum_{i=1}^{n}c_ie^{-\lambda_i\xi}([B^2]-\lambda_i[B^1])\{\phi_i\}). \tag{5.14}$$

6 Numerical examples

The primary goal of this paper is to provide a new static solution for the horizontal layered piezoelectric bounded domain. To illustrate the accuracy and wide applicability of the modified SBFEM for static problem, four numerical examples are investigated. In Section 6.1, the accuracy of proposed method is verified by a two layered model with boundary force and side face load. By comparing with the finite element solutions, the newly developed method is valid for the piezoelectric medium with complex load condition. It illustrates the modified SBFEM can successfully solve the static analysis of bounded domain with boundary force and side face load. In Section 6.2, the influence of side face load acting direction and depth on multilayered piezoelectric model is considered. In Section 6.3, the effect of side face load form on three layered piezoelectric model is analyzed. The varying side face load is firstly introduced in modified SBFEM. Finally, the complex load combinations are addressed for bounded domain. A single layer piezoelectric model with the combined action of elastostatic force and electric force is analyzed. The influence of electric force acting depth is investigated.

6.1 Two layers piezoelectric model with boundary load and side face load

In order to prove the accuracy of proposed method in modeling layered bounded domain, a two layered bounded domain with rigid bottom is investigated. The total model thickness is $b=1$m, each layer thickness is $h_1=h_2=0.5b$, and model width is $2r=6b$. The material coefficients are given as: layer 1: PZT-4 and layer 2: PZT-5H1 as described in Table 1. c_{ij}, e_{ij} and p_{ij} are the elastic constants, piezoelectric constants and permittivity, respectively. The unit of c_{ij}, e_{ij} and p_{ij} are 10^9Nm^{-2}, 1.0Cm^{-2} and 10^{-9}Fm^{-1}, respectively. Six three-node line elements are used for the right and left boundaries, respectively. The plane strain state is considered in this paper. As shown in Figs. 3(a), (b) and (c), the horizontal uniform force and side face load subject on right boundary, left boundary and top side face, respectively. The amplitude of boundary load and side face load are given as $P_1=P_2=P_3=1$. The finite element solutions are computed as the reference solutions. For the two layered piezoelectric model in Fig. 3(a), the node and element numbers for the proposed method and finite element method are listed in Table 2. The finite element model mesh is described in Fig. 4. Only the right/left boundaries of model need to disperse, as shown in Fig. 1. Comparing the finite element mesh (Fig. 4) with the SBFEM mesh (Fig. 1), the obvious advantages of proposed method in meshing can be found. For the boundary load model in Fig. 3(a), the vertical displacement and electric potential results of the points on $x=-3$ axis and $y=0$ axis are compared in Fig. 5, respectively. For further explain the accuracy of proposed method, the results of side face load model in Fig. 3(b) are shown in Fig. 6, respectively. Meanwhile, the vertical displacements of typical points are listed in Table 2. The CPU computation times for two methods (an Intel i7-Core 4 Duo-platform at 3.4GHz with 8-GB RAM) are also given in Table 2. According to Table 2 and Figs. 5-6, it is noted that the proposed method can achieve excellent accuracy. The proposed method has higher efficiency and convergence with fewer nodes and

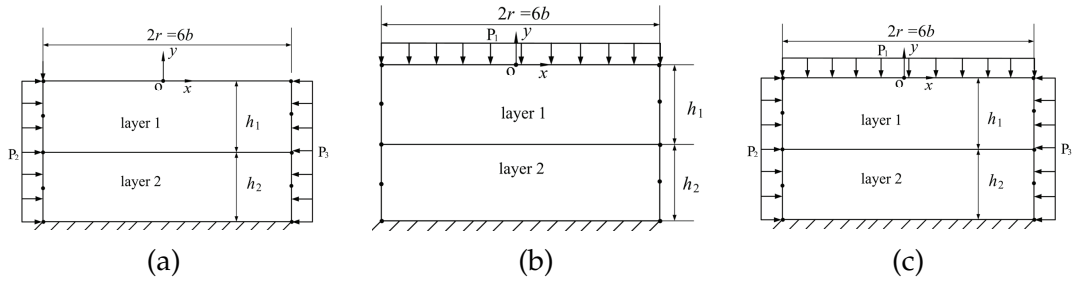

Figure 3: Two layers piezoelectric layer bounded domain. (a) case 1 (b) case 2 (c) case 3.

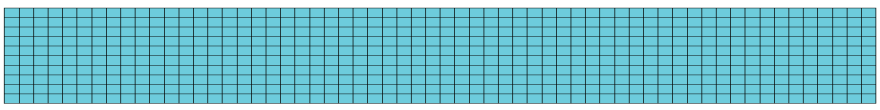

Figure 4: The mesh of finite element model.

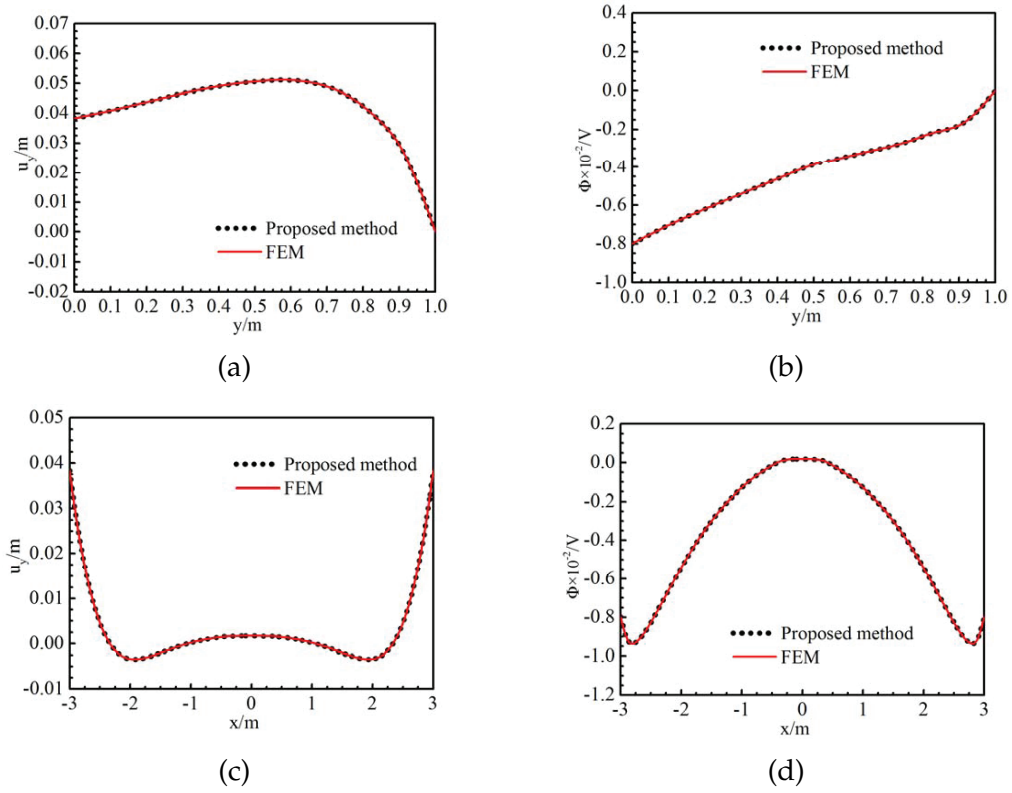

Figure 5: Comparison of the vertical displacement and electric potential results by the proposed method and FEM ((a), (b) are for the points on $x=-3$ axis; (c), (d) are for the points on $y=0$ axis) (case 1) (a) vertical displacement u_y, (b) electric potential ϕ, (c) vertical displacement u_y, (d) electric potential ϕ.

Table 1: Material constants of the piezoelectric materials.

	c_{11}	c_{13}	c_{33}	c_{44}	e_{31}	e_{33}	e_{15}	p_{11}	p_{33}
PZT-4	139	74.3	113	25.6	-6.98	13.84	13.44	6.0	5.47
PZT-5H1	126	84.1	117	23	-6.5	23.3	17.44	15.03	13.0

less computation times. To consider the influence of different loads (in Fig. 3), the results of three load cases are described in Fig. 7. It can be seen from the figure that the load type has great influence on vertical displacement and electric potential in vertical direction. While the side face load has less effect on the displacement and electric potential in horizontal direction.

6.2 Influence of the side face load acting direction and depth

The layered piezoelectric medium usually acts on the complicate load conditions in the most cases. The displacement and electric potential appear different change trends. There-

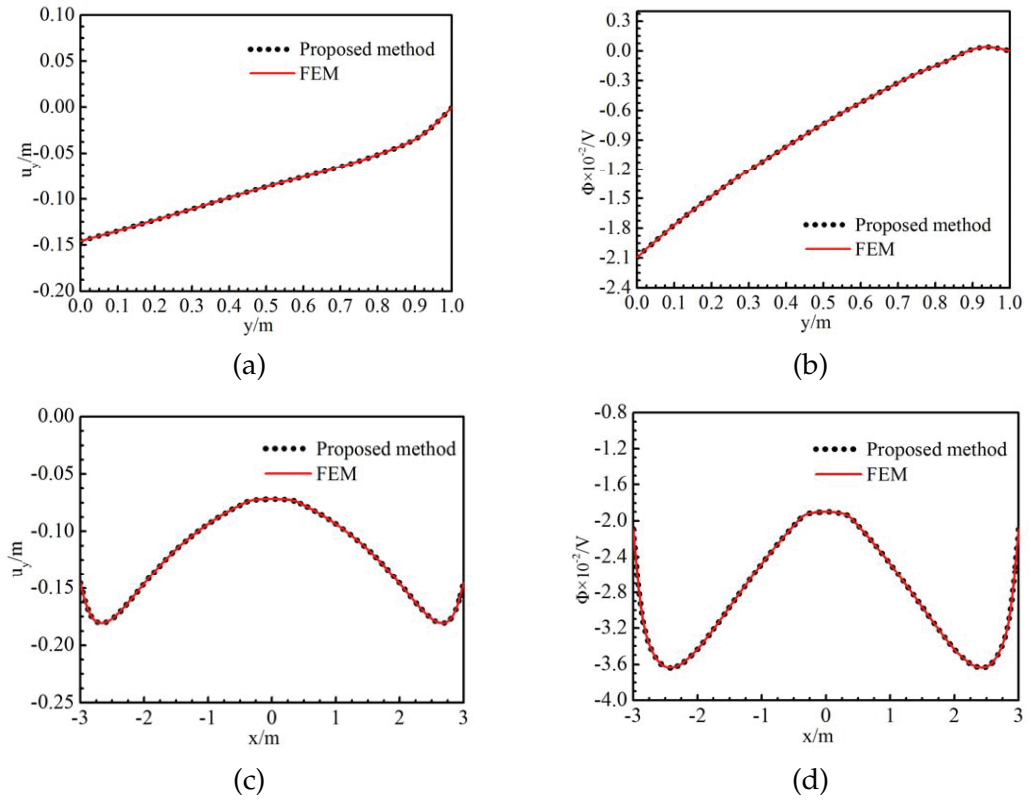

Figure 6: Comparison of the vertical displacement and electric potential results by the proposed method and FEM ((a), (b) are for the points on $x=-3$ axis; (c), (d) are for the points on $y=0$ axis) (case 2) (a) vertical displacement u_y, (b) electric potential ϕ, (c) vertical displacement u_y, (d) electric potential ϕ.

Table 2: Comparison of the proposed method and FEM in vertical displacement u_y of nodes.

		FEM (mesh1)	FEM (mesh2)	FEM (mesh3)	Modified SBFEM (mesh 1)	Modified SBFEM (mesh 2)	Modified SBFEM (mesh 3)
Case 1	Node number	733	1265	1941	10	18	26
	Element number	216	384	600	4	8	12
	Node(-3.00,-0.25)	-0.10581	-0.11028	-0.11694	-0.09842	-0.10248	-0.11693
	Node(-3.00,-0.75)	-0.04471	-0.05147	-0.05898	-0.03940	-0.04362	-0.05896
	Node (-2.52,0.00)	-0.16527	-0.17133	-0.17808	-0.15283	-0.16261	-0.17805
	Node (-1.38,0.00)	-0.09618	-0.10258	-0.10976	-0.08749	-0.09627	-0.10973
	CPU time (s)	7.527	13.637	15.739	0.372	0.593	0.964
Case 2	Node number	733	1265	1941	10	18	26
	Element number	216	384	600	4	8	12
	Node(-3.00,-0.25)	-0.06169	-0.06738	-0.07171	-0.05893	-0.06372	-0.07168
	Node(-3.00,-0.75)	-0.00816	-0.00982	-0.01185	-0.00865	-0.00916	-0.01183
	Node (-2.52,0.00)	-0.16263	-0.16947	-0.17298	-0.15845	-0.16374	-0.17295
	Node (-1.38,0.00)	-0.10563	-0.10968	-0.11117	-0.09657	-0.10635	-0.11115
	CPU time (s)	8.591	14.837	16.159	0.429	0.628	1.236

fore, it is meaningful to discuss the response of multilayered piezoelectric model with different side face loads. A three layered piezoelectric models with different side face load acting directions are considered in Fig. 8. Three side face load cases are given as follows: case 1: horizontal uniform load $P_x=1$ (Fig. 6(a)); case 2: vertical uniform load

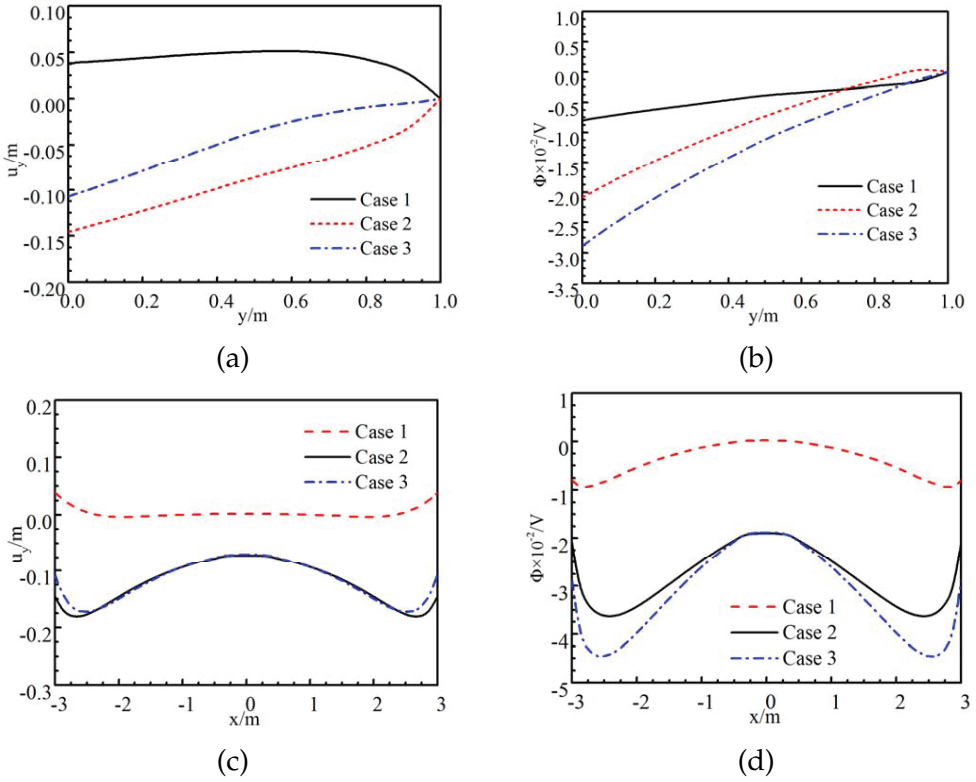

Figure 7: The vertical displacement and electric potential results with different loads ((a), (b) are for the points on $x=-3$ axis; (c), (d) are for the points on $y=0$ axis) (a) vertical displacement u_y, (b) electric potential ϕ, (c) vertical displacement u_y, (d) electric potential ϕ.

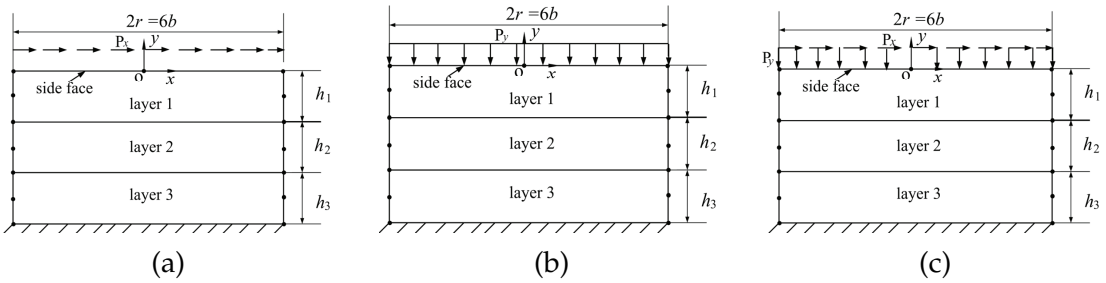

Figure 8: Three layers models with different side face load directions. (a) horizontal uniform load, (b) vertical uniform load, (c) Combination action of the vertical and horizontal uniform loads.

$P_y=1$ (Fig. 6(b)); case 3: the combination of vertical $P_y=1$ and horizontal uniform loads $P_x=1$ (Fig. 6(c)). The three layers material are presented as follows, layer 1 with PZT-4, layer 2 with PZT-5H1 and layer 3 with PZT-6B. And the piezoelectric material parameters are listed in Table 3. The geometry dimensions of three models are the same as those of

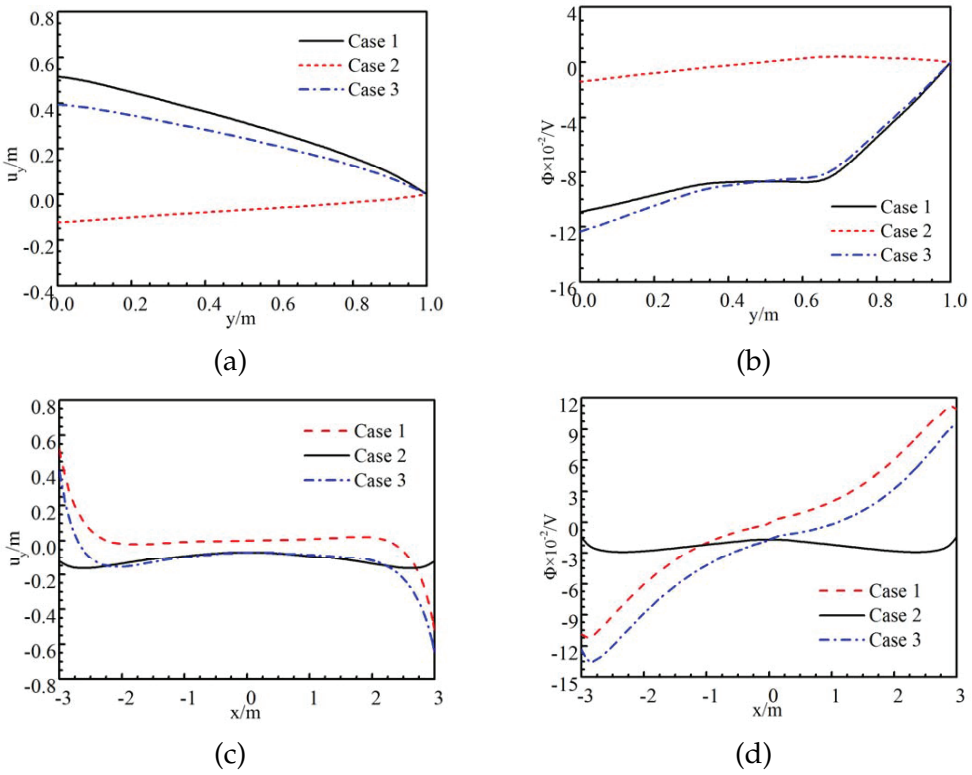

Figure 9: The influence of load direction on the results of three layers piezoelectric model ((a), (b) are for the points on $x=-3$ axis; (c), (d) are for the points on $y=0$ axis) (a) vertical displacement u_y, (b) electric potential ϕ, (c) vertical displacement u_y, (d) electric potential ϕ.

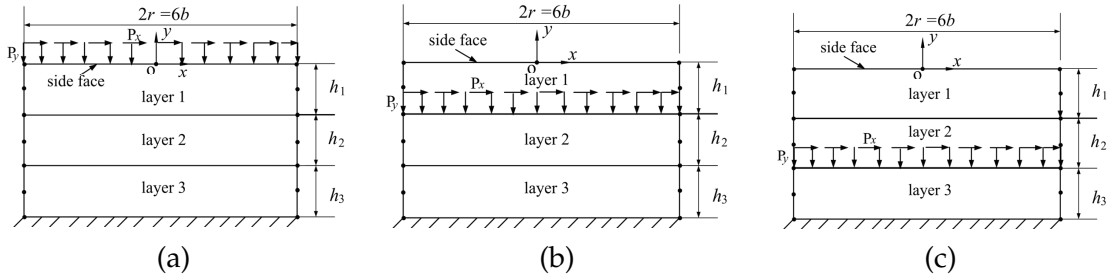

Figure 10: Three piezoelectric layers bounded domain subjected to x and y directions side face loads in different depths. (a) case 1, (b) case 2, (c) case 3.

Section 6.1. The total thickness is equal to $b=1$m, each layer thickness is $h_1=h_2=h_3=1/b$, and the model width is $2r=6b$. As shown in Fig. 9, the vertical displacement and electric potential with different loads are analyzed. It can be observed from Fig. 9 that the differences between the amplitudes of vertical displacement and electric potential for case

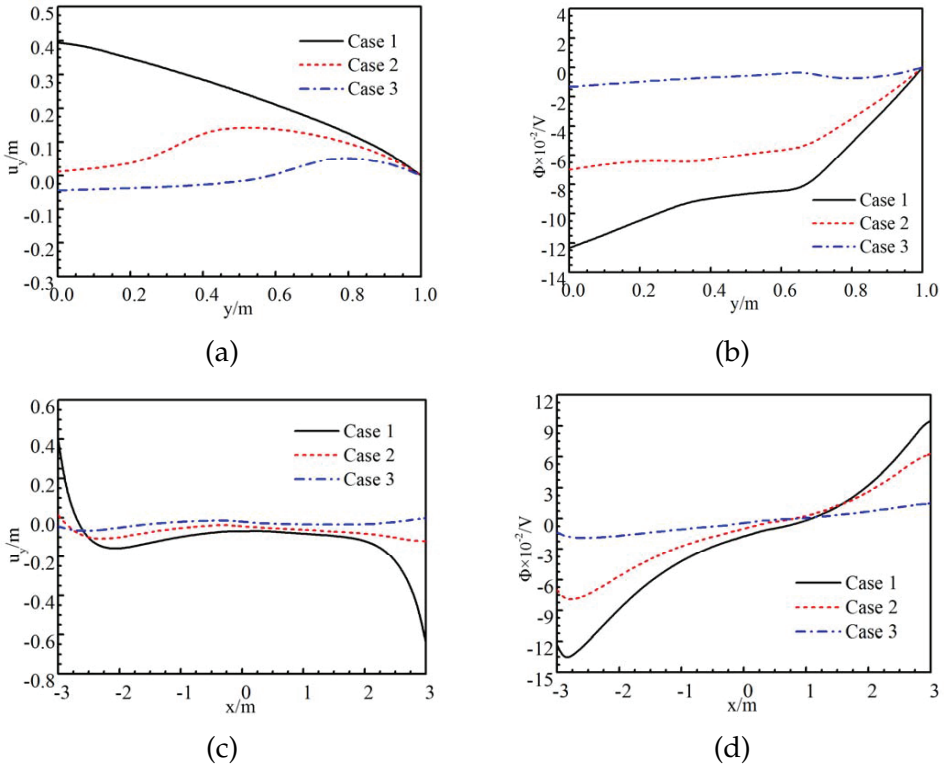

Figure 11: The influence of load depth on the results of three layers piezoelectric model ((a), (b) are for the points on $x=-3$ axis; (c), (d) are for the points on $y=0$ axis) (a) vertical displacement u_y, (b) electric potential ϕ, (c) vertical displacement u_y, (d) electric potential ϕ.

2 and case 3 are relatively small, except for the electric potential of the points on $y=0$ axis. Then, the complex side face loads case which act on the x and y directions in different depths are considered, as shown in Fig. 10. The results of three layered piezoelectric bounded domain are plotted in Fig. 11. From the figure, when the depth increases, the vertical displacement of the points in vertical direction decreases. And the opposite phenomenon can be found for the electric potential results. There is no significant influence on the vertical displacement of the horizontal direction points with varying load depth. The electric potential of horizontal direction points decreases with load depth increases.

Table 3: Material constants of the piezoelectric materials.

	c_{11}	c_{13}	c_{33}	c_{44}	e_{31}	e_{33}	e_{15}	p_{11}	p_{33}
PZT-4	139	74.3	113	25.6	-6.98	13.84	13.44	6.00	5.47
PZT-5H1	126	84.1	117	23.0	-6.50	23.3	17.44	15.03	13.0
PZT-6B	168	60	163	27.1	-0.90	7.1	4.60	3.60	3.40

6.3 Influence of the side face load form on the multilayered piezoelectric model

As shown in Fig. 12, a three layered model is calculated by considering different side face load forms. The study aim in this section is to reveal the fact that side face load form can obviously influence the static results of piezoelectric layered model. The physical dimensions of three layered model are given as: total model thickness is $b=1$m, model width is $2r=6b$, thickness of each layer is $b/3$. The piezoelectric material parameters of each layer are: layer 1 with PZT-4; layer 2 with PZT-5H1; layer 3 with PZT-6B, as listed in Table 3. As described above, the definition formulation of side face load is given in Eq. (5.2). For the fixed radial coordinate ξ, the side face load depends on arbitrary constant t. When $t=0$, the side face load is a constant load and the solution form can be obtain easily. Thus, the load form with $t=0$ case is applied to many examples about side face problem. However, the practical load is not always constant. In this section, the side face load with $t=1$ is firstly considered for the horizontal layered model. Then, the varying side face loads with $t=1,2,3$, and constant side face load with $t=0$ are plotted in Fig. 13. The layered piezoelectric bounded domain with varying side face load is analyzed as shown

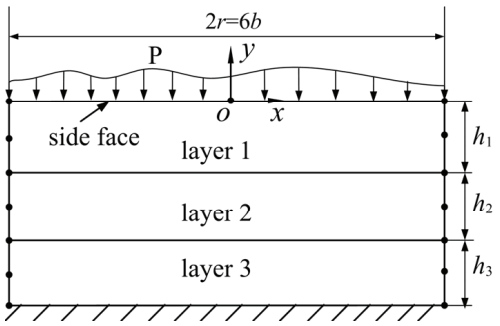

Figure 12: Three layers piezoelectric bounded domain subjecting on varying distributed side face load.

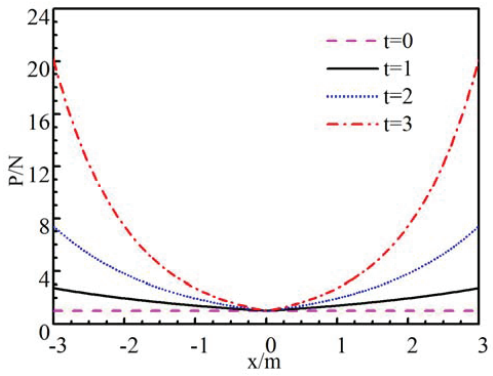

Figure 13: Different side face load forms.

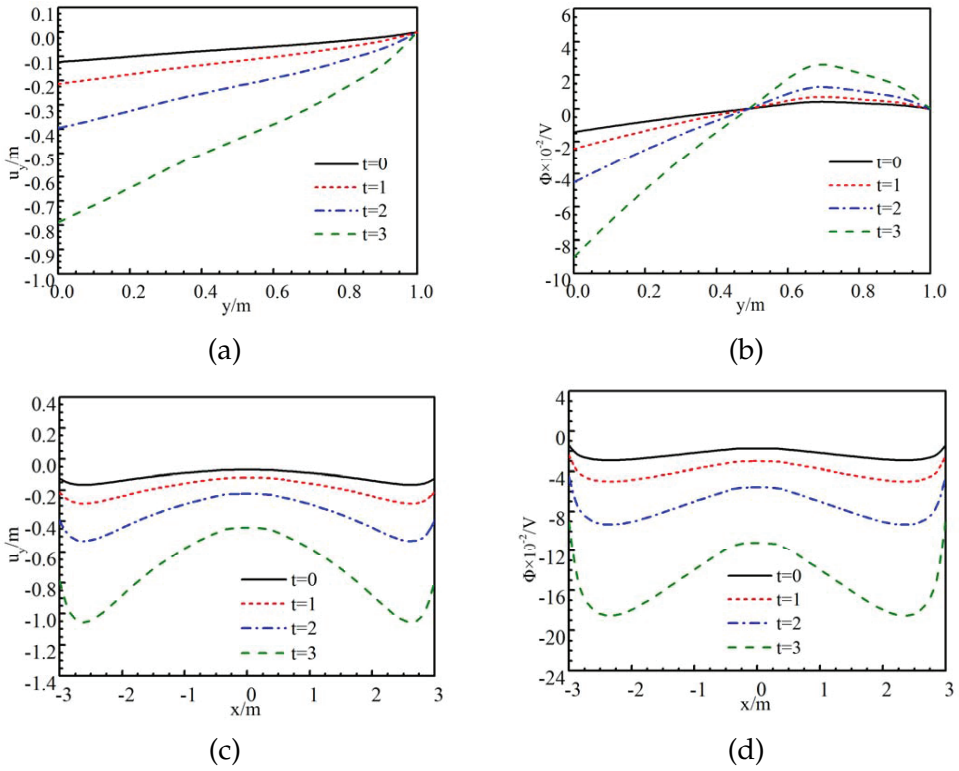

Figure 14: The influence of load form on the results of three layers piezoelectric model ((a), (b) are for the points on $x=-3$ axis; (c), (d) are for the points on $y=0$ axis) (a) vertical displacement u_y, (b) electric potential ϕ, (c) vertical displacement u_y, (d) electric potential ϕ.

in Fig. 14. It can be seen from Fig. 14 that the vertical displacement and electric potential decrease with arbitrary constant t increases. Secondly, for the fixed value $t=1$, the side face loads acts on three layered model (Fig. 12) in different depths as shown in Fig. 15. Three acting depths are considered as: case 1 with 0, case 2 with $b/3$, and case 3 with $2b/3$. According to the charge trends shown in Fig. 16, the influence of load depth on vertical displacement and electric potential is significant. The conclusion can be obtained that larger depth leads to the bigger vertical displacement and electric potential.

6.4 Influence of the action depth of electric side face load

According to the characteristic of piezoelectric medium, the results of the model with complex side face loads reveals different mechanical and electrical properties. In this section, a five layered piezoelectric bounded domain subjects the combination elastic force P_1 and electric force P_2. As shown in Fig. 17, the total layer thickness is $b=1$m, and the model width is $2r=6b$, and each layer thickness is $h_1=h_2=h_3=h_4=b/3$, $h_5=b/3$. The piezoelectric material for each layer is listed in Table 4: layer 1 with PZH-5H1, layer 2

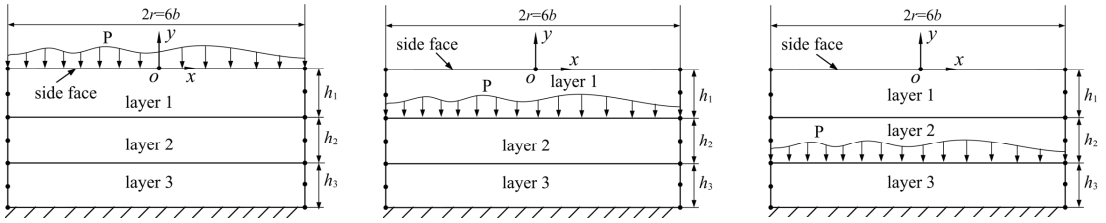

Figure 15: Varying side face load acts on different depths on the three layers model. (a) case 1, (b) case 2, (c) case 3.

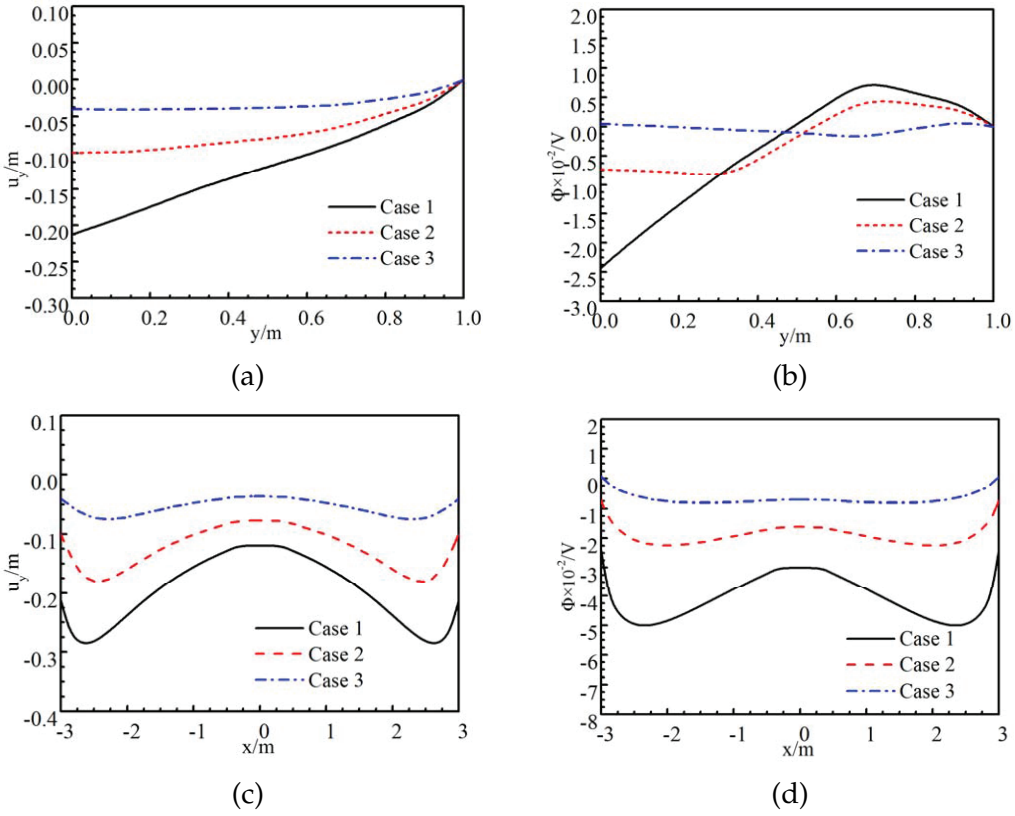

Figure 16: The influence of load depth on the results of three layers piezoelectric model ((a), (b) are for the points on $x=-3$ axis; (c), (d) are for the points on $y=0$ axis) (a) vertical displacement u_y, (b) electric potential ϕ, (c) vertical displacement u_y, (d) electric potential ϕ.

with InN, layer 3 with PZH-4, layer 4 with GaN and layer 5: AIN. As shown in Fig. 16, the uniform elastic force $P_1=1$ throughout acts on the surface line with $y=0$, and the uniform electric force $P_2=1$ acts on different depths. Three electric force action depths are considered in this example, case 1: 0, case 2: $b/3$, and case 3: $2b/3$. The vertical

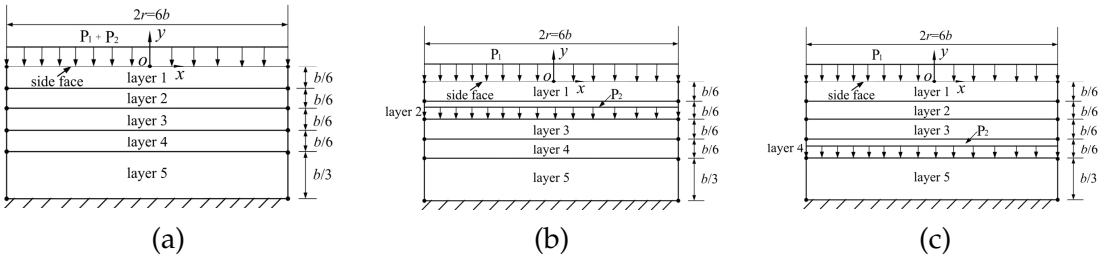

Figure 17: Five layers piezoelectric model with different action depth of the electric force. (a) case 1, (b) case 2, (c) case 3.

displacements and electric potential are described in Fig. 16. The vertical displacement increases and electric potential decreases with the increase of electric force acting depth.

6.5 Practical application on the road system

To illustrate the practicability of proposed method, the road system is solved in this section. As shown in Fig. 19, the piezoelectric layer lies on the road foundation. Two vehicle loads q_1 and q_2 subject on the right and left road surfaces, respectively. The acting widths are $l_1 = 2b$ and $l_2 = 2b$. The piezoelectric layer thickness is $h = b$, and total road width is $2r = 6b$. The PZH-5H[1] piezoelectric material parameters are given in Table 4. The left vehicle load is $q_1 = 1.0\times10^9$N. In order to discuss the influence of vehicle load distribution, three right vehicle loads q_2 are considered as follows: 0.5×10^9N, 1.0×10^9N and 1.5×10^9N. The vertical displacements of the points on $x=0$ and $y=0$ axes for different vehicle loads are plotted in Fig. 20. For the points on $x=0$ axis, the general trend of vertical displacements is weaken with depth increase as plotted in Fig. 18(a). The enhanced right vehicle load leads to bigger displacement. The vertical displacements of surface points are given in Fig. 20(b). As expected, the results increase with right vehicle load enhances, and the main influence area exists in the right change load segment. Because the difference between two vehicle loads is weaken, the influence of different vehicle loads trends to disappear.

Table 4: Material constants of the piezoelectric materials.

	c_{11}	c_{13}	c_{33}	c_{44}	e_{31}	e_{33}	e_{15}	p_{11}	p_{33}
PZT-5H[1]	126	84.1	117	23	-6.5	23.3	17.44	15.03	13.0
InN	190	121	182	10	-0.57	0.97	-0.22	0.1355	0.1355
PZT-4	139	74.3	113	25.6	-6.98	13.84	13.44	6.0	5.47
GaN	390	106	398	105	-0.33	0.65	-0.30	0.0788	0.0788
AIN	410	99	389	125	-0.58	1.55	-0.48	0.0753	0.0753

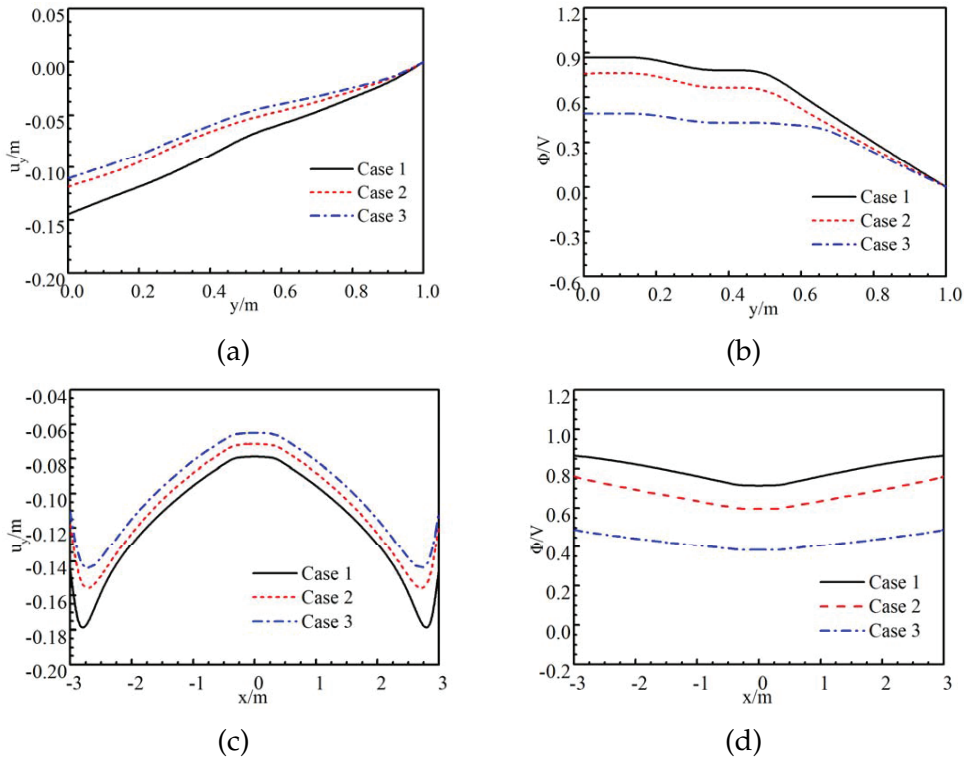

Figure 18: The influence on the action depth of electric force in the five layers combination model ((a), (b) are for the points on $x=-3$ axis; (c), (d) are for the points on $y=0$ axis), (a) vertical displacement u_y, (b) electric potential ϕ, (c) vertical displacement u_y, (d) electric potential ϕ.

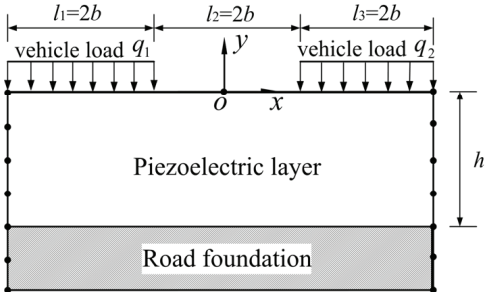

Figure 19: The piezoelectric layer on the road foundation with different vehicular loads.

7 Conclusions

In this paper, a new technology the modified SBFEM which is used to model the static problem for the layered piezoelectric bounded domain is proposed. Based on the Hamilton system, the Duality theory is introduced to derive the modified SBFEM governing

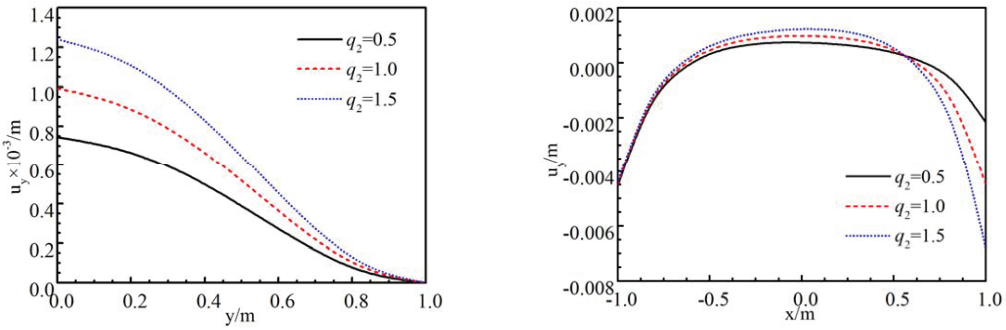

(a) (b)

Figure 20: The vertical displacement u_y of the observation points for different vehicular loads (a) the points on $x=0$ axis, (b) the points on $y=0$ axis.

equation with piezoelectric medium. The Hamilton derivation technology makes solving progress be concise. Then, the eigenvalue decomposition method is introduced to solve the modified SBFEM equation with piezoelectric medium. The generalized displacement and node forces can be expressed as power exponent function with radial coordinate by introducing the auxiliary variable. A novel static solution forms for the layered piezoelectric bounded domain are obtained. The inner displacement and electric charge in bounded domain can be computed through interpolating boundary value. For the special load case, the side face load can be expressed as the power exponent function with radial coordinate. The static solution forms are given for a newly side face load form which is quit suitable for horizontal layered bounded domain. It is a new formulation for the static analysis of layered piezoelectric bounded domain. This technique significantly extends the modified SBFEM application range in modelling elastostatic problems. The propose method has high convergence rate and efficiency, excellent accuracy characteristics. In this method, the exact solutions can be obtained even by less amount of computation time and fewer discretized boundary nodes. The numerical results also show that the increasement of depth leads to the vertical displacement for vertical direction points weaken. However, the opposite phenomenon can be found for the electric potential in vertical direction. It can be noted that the load depth has an insignificant influence on the vertical displacement in horizontal direction. The electric potential in horizontal direction decreases with load depth increases. The influence of load acting depth on vertical displacement and electric potential is significant. The larger depth leads to the bigger vertical displacement and electric potential. The vertical displacement increases and electric potential decreases with the electric force acting depth increases. At last, the proposed method is applied to solve road system. The change trend of vertical displacement causing by vehicle loads are given, and the influence of different vehicle loads is discussed.

Acknowledgements

This research was supported by Grants Nos. 51409038, 51421064, 51138001 and 51308307 from the National Natural Science Foundation of China, Grant No. GZ1406 from the Open Foundation of State Key Laboratory of Structural Analysis for Industrial Equipment, Grant No. DUT15RC(4)23 from the fundamental research funds for the central universities, and Grant No. YL1610 from the Youth Foundation of State Key Laboratory of Coastal and Offshore Engineering for which the authors are grateful.

References

[1] N. Abd Aziz, B. Bais, M. R. Buyong, B. Y. Majlis and A. N. Nordin, *FEM analysis of wavelength effects in piezoelectric substrate,* Semiconductor Electronics (ICSE), 2014 IEEE International Conference on IEEE, (2014), pp. 259–262.

[2] R. M. S. Abu, M. Shohel and V. H. Bill, *A comprehensive review on vibration based micro power generators using electromagnetic and piezoelectric transducer mechanisms,* Energy Conversion and Management, 106 (2015), pp. 728–747.

[3] S. D. Akbarov and N. Ilhan, *Time-harmonic Lamb's problem for a system comprising a piezoelectric layer and piezoelectric half-plane,* J. Sound Vib., 332(21) (2013), pp. 5375–5392.

[4] R. A. Alashti, M. Khorsand and M. H. Tarahhomi, *Thermo-elastic analysis of a functionally graded spherical shell with piezoelectric layers by differential quadrature method,* Scientia Iranica, 20(1) (2013), pp. 109–119.

[5] M. H. Bazyar and C. M. Song, *Transient analysis of wave propagation in non-homogeneous elastic unbounded domains by using the scaled boundary finite-element method,* Earthquake Engineering and Structural Dynamics, 35(14) (2006), pp. 1787–1806.

[6] R. K. Bhangale and N. Ganesan, *Static analysis of simply supported functionally graded and layered magneto-electro-elastic plates,* Int. J. Solids Structures, 43(10) (2006), pp. 3230–3253.

[7] C. Birk and R. Behnke, *A modified scaled boundary finite element method for three-dimensional dynamic soil-structure interaction in layered soil,* Int. J. Numer. Methods Eng., 89(3) (2012), pp. 371–402.

[8] X. Cao, F. Jin, I. Jeon and T. J. Lu, *Propagation of love waves in a functionally graded piezoelectric material (FGPM) layered composite system,* Int. J. Solids Structures, 46(22) (2009), pp. 4123–4132.

[9] A. Chakraborty, S. Gopalakrishnan and E. Kausel, *Wave propagation analysis in inhomogeneous piezo-composite layer by the thin-layer method,* Int. J. Numer. Methods Eng., 64(5) (2005), pp. 567–598.

[10] A. L. Chen, D. J. Yan, Y. S. Wang and C. Zhang, *Anti-plane transverse waves propagation in nanoscale periodic layered piezoelectric structures,* Ultrasonics, 65 (2016), pp. 154–164.

[11] K. Chen, D. Zou, X. Kong, A. Chan and Z. Hu, *A novel nonlinear solution for the polygon scaled boundary finite element method and its application to geotechnical structures,* Comput. Geotech., 82 (2017), pp. 201–210.

[12] L. Chen, Y. W. Zhang, G. R. Liu, H. Nguyen-Xuan and H. Z. Zhang, *A stabilized finite element method for certified solution with bounds in static and frequency analyses of piezoelectric structures*, Comput. Methods Appl. Mech. Eng., 241 (2012), pp. 65–81.

[13] X. CHEN, C. BIRK AND C. M. SONG, *Transient analysis of wave propagation in layered soil by using the scaled boundary finite element method,* Comput. Geotech., 63 (2015), pp. 1–12.
[14] S. CHEN, T. TANG AND Z. WANG, *Shear-horizontal acoustic wave propagation in piezoelectric bounded plates with metal gratings,* The Journal of the Acoustical Society of America, 117(6) (2005), pp. 3609–3615.
[15] J. M. DE OLIVEIRA BARBOSA, E. KAUSEL, Á. AZEVEDO AND R. CALCADA, *Formulation of the boundary element method in the wavenumber-frequency domain based on the thin layer method,* Comput. Structures, 161 (2015), pp. 1–16.
[16] A. J. DEEKS, *Prescribed side-face displacements in the scaled boundary finite element method,* Comput. Structures, 82(15) (2004), pp. 1153–1165.
[17] A. J. DEEKS AND J. P. WOLF, *A virtual work derivation of the scaled boundary finite-element method for elastostatics,* Comput. Mech., 28(6) (2002), pp. 489–504.
[18] J. DU, K. XIAN, Y. K. YONG AND J. WANG, *SH-SAW propagation in layered functionally graded piezoelectric material structures loaded with viscous liquid,* Acta Mech., 2010, 212(3-4) (2010), pp. 271–281.
[19] I. ESHRAGHI AND A. YOUSEFI-KOMA, *Static analysis of a functionally graded piezoelectric beam using finite element method,* ASME 2010 10th Biennial Conference on Engineering Systems Design and Analysis, American Soc. Mech. Eng., (2010), pp. 503–510.
[20] X. Q. FANG, J. X. LIU, X. H. WANG, T. ZHANG AND S. ZHANG, *Dynamic stress from a cylindrical inclusion buried in a functionally graded piezoelectric material layer under electro-elastic waves,* Composites Sci. Tech., 69(7) (2009), pp. 1115–1123.
[21] A. FERNANDES AND J. POUGET, *Analytical and numerical approaches to piezoelectric bimorph*, Int. J. Solids Structures, 40(17) (2003), pp. 4331–4352.
[22] M. FERI, A. ALIBEIGLOO AND A. A. A. P. ZANOOSI, *Three dimensional static and free vibration analysis of cross-ply laminated plate bonded with piezoelectric layers using differential quadrature method,* Meccanica, (2015), pp. 1–17.
[23] I. K. FONTARA, F. WUTTKE, T. RANGELOV AND P. DINEVA, *A non-conventional BEM for seismic wave propagation in continuously inhomogeneous half-plane,* Numer. Method Geotech. Eng. Hick, Brinkgreve & Rohe, 1 (2014), pp. 367–372.
[24] S. K. HA AND Y. H. KIM, *Analysis of a piezoelectric multimorph in extensional and flexural motions,* J. Sound Vib., 253(5) (2002), pp. 1001–1014.
[25] M. S. ISLAM, M. AHMED AND M. M. UDDIN, *Numerical investigation of singularity at a vertex in 3D transversely isotropic piezoelectric bonded joints by FEM,* Electrical Information and Communication Technology (EICT), 2013 International Conference on, IEEE, (2014), pp. 1–5.
[26] S. KAPURIA, *An efficient coupled theory for multilayered beams with embedded piezoelectric sensory and active layers,* Int. J. Solids Structures, 38(50) (2001), pp. 9179–9199.
[27] B. JOE AND D. STEVE, *Piezoelectric nanogenerators-a review of nanostructured piezoelectric energy harvesters,* Nano Energy, 14 (2015), pp. 15–29.
[28] X. KANG AND S. DONG, *Response of piezoelectric laminated micro plates under the excitation of an ultrasonic wave,* Seventh International Symposium on Precision Mechanical Measurements, International Society for Optics and Photonics, (2016), 99031U-99031U-7.
[29] E. KAUSEL, *Thin-layer method: formulation in the time domain,* Int. J. Numer. Methods Eng., 37 (1994), pp. 927–941.
[30] Y. KOUTSAWA, G. GIUNTA AND S. BELOUETTAR, *Hierarchical FEM modelling of piezo-electric beam structures,* Composite Structures, 95 (2013), pp. 705–718.
[31] K. Y. LAM, X. Q. PENG, G. R. LIU AND J. N. REDDY, *A finite-element model for piezoelectric composite laminates,* Smart Materials Structures, 6(5) (1997), pp. 583.

[32] M. LEZGY-NAZARGAH, *Efficient coupled refined finite element for dynamic analysis of sandwich beams containing embedded shear-mode piezoelectric layers,* Mech. Adv. Materials Structures, 23(3) (2016), pp. 337–352.
[33] C. LI, H. MAN, C. M. SONG AND W. GAO, *Fracture analysis of piezoelectric materials using the scaled boundary finite element method,* Eng. Fracture Mech., 97 (2013), pp. 52–71.
[34] C. LI AND L. TONG, *A mixed SBFEM for stress singularities in nearly incompressible multi-materials,* Comput. Structures, 157 (2015), pp. 19–30.
[35] X. LI AND M. WANG, *Three-dimensional Green's functions for infinite anisotropic piezoelectric media,* Int. J. Solids Structures, 44(5) (2007), pp. 1680–1684.
[36] R. L. LIN, *Full-field analysis of three dimensional piezoelectric layered half-space with point loading,* Euro. J. Mech. A Solids, 42 (2013), pp. 158–175.
[37] L. LIU, Y. PAN AND Z. ZHONG, *The study of P-SV wave propagation in the periodic piezoelectric layered material,* Piezoelectricity, Acoustic Waves and Device Applications (SPAWDA), Symposium on, IEEE, (2013), pp. 1–5.
[38] C. C. MA AND J. M. LEE, *Theoretical analysis of generalized loadings and image forces in a planar magnetoelectroelastic layered half-plane,* J. Mech. Phys. Solids, 57(3) (2009), pp. 598–620.
[39] K. MORI, Y. SHINDO AND F. NARITA, *Dynamic electromagnetomechanical behavior of clamped-free giant magnetostrictive/piezoelectric laminates under AC electric fields,* Smart Materials Structures, 21 (2012), 115003.
[40] J. P. NOWACKI, V. I. ALSHITS AND A. RADOWICZ, *The Green's functions for an infinite piezoelectric strip with line sources at the surfaces,* Int. J. Appl. Electromagn. Mech., 12 (2000), pp. 177–202.
[41] J. P. NOWACKI, V. I. ALSHITS AND A. RADOWICZ, *2D electro-elastic fields in a piezoelectric layer-substrate structure,* Int. J. Eng. Sci., 40 (2002), pp. 2057–2076.
[42] E. PAN AND F. G. YUAN, *Three-dimensional Green's functions in anisotropic piezoelectric bimaterials,* Int. J. Eng. Sci., 38 (2000), pp. 1939–1960.
[43] Z. QIU, X. ZHANG AND X. ZHANG, *A vision-based vibration sensing and active control for a piezoelectric flexible cantilever plate,* J. Vib. Control, 22(5) (2014), pp. 1320–1337.
[44] M. C. RAY, R. BHATTACHARYA AND B. SAMANTA, *Exact solutions for static analysis of intelligent structures,* AIAA J., 31(9) (1993), pp. 1684–1691.
[45] M. C. RAY, R. BHATTACHARYA AND B. SAMANTA, *Exact solutions for dynamic analysis of composite plates with distributed piezoelectric layers,* Comput. Structures, 66(6) (1998), pp. 737–743.
[46] J. N. REDDY, Mechanics of Laminated Composite Plates: Theory and Analysis, CRC Press, 1997.
[47] D. RESTREPO, J. D. GÓMEZ, AND J. D. JARAMILLO, *SH wave number Green's function for a layered, elastic half-space, Part I: Theory and dynamic canyon response by the discrete wave number boundary element method,* Pure Appl. Geophys., 171(9) (2014), pp. 2185–2198.
[48] P. K. SAROJ, S. A. SAHU, S. CHAUDHARY AND A. CHATTOPADHYAY, *Love-type waves in functionally graded piezoelectric material (FGPM) sandwiched between initially stressed layer and elastic substrate,* Waves in Random and Complex Media, 25(4) (2015), pp. 608–627.
[49] S. H. SEALE AND E. KAUSEL, *Point loads in cross-anisotropic layered half spaces,* J. Eng. Mech., 115 (1989), pp. 509–542.
[50] C. M. SONG AND J. P. WOLF, *The scaled boundary finite-element method-alias consistent infinitesimal finite-element cell method-for elastodynamics,* Comput. Methods Appl. Mech. Eng., 147 (1997), pp. 329–344.
[51] N. M. SYED AND B. K. MAHESHWARI, *Modeling using coupled FEM-SBFEM for three-*

dimensional seismic SSI in time domain, Int. J. Geomech., 14(1) (2014), pp. 118–129.
[52] A. TADEU, J. ANTÓNIO, L. GODINHO AND N. SIMOES, *Boundary element method analyses of transient heat conduction in an unbounded solid layer containing inclusions,* Comput. Mech., 34(2) (2004), pp. 99–110.
[53] H. F. TIERSTEN, Linear Piezoelectric Plate Vibrations: Elements of the Linear Theory of Piezoelectricity and the Vibrations Piezoelectric Plates, Springer, 2013.
[54] H. S. TZOU AND H. F. TIERSTEN, *Elastic analysis of laminated composite plates in cylindrical bending due to piezoelectric actuators,* Smart Materials Structures, 1994, 3(3) (1994), pp. 255–265.
[55] S. Y. WANG, Active Vibration Control of Smart Piezoelectric Composite Plates, Ph.D. Dissertation, National University of Singapore, Singapore, 2002.
[56] B. L. WANG AND J. E. LI, *Hyperbolic heat conduction and associated transient thermal fracture for a piezoelectric material layer,* Int. Solids Structures, 50(9) (2013), pp. 1415–1424.
[57] W. WANG, Z. GUO, Y. PENG AND Q. ZHANG, *A numerical study of the effects of the T-shaped baffles on liquid sloshing in horizontal elliptical tanks,* Ocean Eng., 111 (2016), pp. 543–568.
[58] W. WANG, Y. PENG, Y. ZHOU AND Q. ZHANG, *Liquid sloshing in partly-filled laterally-excited cylindrical tanks equipped with multi baffles,* Appl. Ocean Res., 59 (2016), pp. 543–563.
[59] W. WANG, G. TANG, X. SONG AND Y. ZHOU, *Transient sloshing in partially filled laterally excited horizontal elliptical vessels with T-shaped baffles,* J. Pressure Vessel Tech., 139(2) (2017), 021302.
[60] H. XU, D. ZOU, X. KONG AND X. SU, *Error study of Westergaard's approximation in seismic analysis of high concrete-faced rockfill dams based on SBFEM,* Soil Dyn. Earthquake Eng., 94 (2017), pp. 88–91.
[61] Z. YANG, *Application of scaled boundary finite element method in static and dynamic fracture problems,* Acta Mech. Sinica, 22(3) (2006), pp. 243–256.
[62] H. J. ZHONG, H. Y. WANG, J. LEI AND W. D. GU, *BEM for static and dynamic fracture analysis in thin piezoelectric structures,* Adv. Materials Res., 816 (2013), pp. 149–152.